

Numerical Relativity and Astrophysics

LUIS LEHNER¹ & FRANS PRETORIUS²

¹*Perimeter Institute for Theoretical Physics,
51 Caroline Street North, Waterloo, Ontario N2L 2Y5, Canada*

²*Department of Physics, Princeton University,
Princeton, New Jersey 08544, USA*

Key Words black holes, neutron stars, gravitational waves, gamma-ray burts,
general relativity

Abstract Throughout the Universe many powerful events are driven by strong gravitational effects that require general relativity to fully describe them. These include compact binary mergers, black hole accretion and stellar collapse, where velocities can approach the speed of light, and extreme gravitational fields $-\Phi_{\text{Newt}}/c^2 \simeq 1-$ mediate the interactions. Many of these processes trigger emission across a broad range of the electromagnetic spectrum. Compact binaries further source strong gravitational wave emission that could directly be detected in the near future. This feat will open up a gravitational wave window into our Universe and revolutionize its understanding. Describing these phenomena requires general relativity, and –where dynamical effects strongly modify gravitational fields– the full Einstein equations coupled to matter sources. Numerical relativity is a field within general relativity concerned with studying such scenarios that cannot be accurately modeled via perturbative or analytical calculations. In this review, we examine results obtained within this discipline, with a focus on its impact in astrophysics.

CONTENTS

Introduction	2
Brief Review of Techniques, Methods and Information Obtainable from Gravitational Waves	3
Brief Description of the Dynamics of a Binary System	4
<i>Properties of Gravitational Wave Emission</i>	5
<i>Priors on Binary Parameters</i>	7
Binary Black Holes	9
<i>Results and Applications of Merger Simulations</i>	10
<i>Further Physics</i>	14
Non-vacuum Binaries	16
<i>Binary Neutron Star Mergers</i>	17
<i>Black hole–neutron star mergers</i>	21
Gravitational Collapse to a Neutron Star or Black Hole	24
Further Frontiers	25

Final Comments	26
Acknowledgements	26

1 Introduction

Strong gravitational interactions govern many of the most fascinating astrophysical phenomena and lie behind some of the most spectacular predictions of general relativity, such as black holes and neutron stars. These objects produce extreme gravitational fields and are believed to be responsible for the most energetic events in our Universe. Indeed, models for gamma-ray bursts, quasars, AGN, pulsars and a class of ultra-high-energy cosmic rays all have these still poorly understood compact objects as putative central engines. Observations across the electromagnetic spectra, soon to be combined with gravitational signals produced by merging binaries, should provide important insights into their nature. Of course, such understanding can only be gained by contrasting theoretical models that include all the relevant physics to the full front of observations.

It is important to distinguish two sub-classes of strongly gravitating systems. The first is where the self-gravitation of any matter/gas/plasma interacting with a compact object or binary is sufficiently weak such that the gravitational back reaction can be ignored or treated perturbatively. Such systems can be analyzed by studying the dynamics of matter on a given fixed background geometry. Examples include accreting black holes and tidal disruption of main sequence stars by supermassive black holes. Widely separated compact binary systems also belong to this sub-class, and suitable post-Newtonian (PN) expansions can be adopted to account for the slowly varying gravitational field and its effects.

By contrast, if the interaction is strong and can fundamentally affect the gravitational field of the system, a fully relativistic, self-gravitating study must be performed. To this end the Einstein equations, coupled to any relevant matter fields, must be employed. This task is complex due to the involved nature of Einstein's equations (a nonlinear, strongly coupled system of equations) in which analytical solutions are only known in highly specialized scenarios. Consequently, numerical simulations are required and the discipline that concentrates on the development and application of numerical solutions of Einstein's equations is known as *numerical relativity* (NR).

This discipline has, over several decades, steadily progressed to the current epoch in which studies of relevance to astrophysics can now be performed that address questions both of fundamental theoretical interest and that make contact with observations¹. Of particular interest, spurred by a hope of imminent gravitational wave observation, are systems capable of producing strong gravitational emission. Detectors include ground-based interferometers such as LIGO/VIRGO/KAGRA (2, 3, 216) targeting the $\simeq 10\text{Hz}$ - 1KHz frequency band, a pulsar timing network (see e.g. (112)) sensitive to the 300pHz - 100nHz window,

¹Numerical relativity is also being used to address problems in cosmological contexts. Applications that require NR, including bubble collisions (116, 229), the issue of nonlinear structures and voids (236, 237, 239), the evolution near the bounce in cyclic models (84, 235) and certain aspects of cosmic string dynamics (132), are still at either a speculative level or being explored. In contrast, the paradigm applicable to most of present day observational cosmology can effectively be addressed with exact Friedman-Lamaitre-Robison-Walker solutions and perturbations about them, and do not require NR.

and possible future spaced-based missions (NGO/eLISA, see, e.g. (7)), sensitive between $\simeq 10\mu\text{Hz}$ - 0.1Hz . Compact binary systems, involving black holes or neutron stars, are the most natural sources and have thus been the focus of most recent efforts (see e.g. (10) for a recent overview). In this article we review the key messages obtained by NR relevant to astrophysics. The discipline is still in the midst of rapid development over an increasing breadth of applications, promising even more exciting future discoveries of astrophysical import.

2 Brief Review of Techniques, Methods and Information Obtainable from Gravitational Waves

Understanding gravity in highly dynamical/strongly gravitating regimes requires solving Einstein's equations. This provides the metric tensor, g_{ab} , which encodes gravitational effects in geometrical terms. The covariant character of the equations encode the equivalence principle, hence there is no preferred frame of reference to write the particular form of the metric for a given physical geometry. This further implies that the field equations determining g_{ab} do not lend themselves to a well defined initial value problem unless the spacetime is foliated into a series of surfaces that provide a notion of "time." One can then cast Einstein's equations in a form that provides a recipe to evolve the intrinsic metric of each slice with time in what has been called "geometrodynamics." There are several options to carry out this program (see, e.g. the discussion by (137)), though the most common one is to define these surfaces to be spacelike. This is also most closely related to Newtonian mechanics, and hence provides useful intuition in astrophysical scenarios; furthermore, with some additional assumptions about the coordinates, the familiar Newtonian potential can easily be extracted from the metric for weakly gravitating systems. Current efforts most commonly employ one of two particular reformulations of Einstein's equations: the generalized harmonic and the BSSN formulations². These equations are hyperbolic with characteristics given by the speed of light (regardless of the state of the system, as opposed to the familiar case of hydrodynamics in which perturbations propagate with speeds tied to the state of the fluid). When coupling in matter sources the equations of relativistic hydrodynamics (or magnetohydrodynamics) on a dynamical, curved geometry must also be considered. The relevant equations can be expressed in a way fully consistent with standard approaches to integrate the Einstein equations (for a review on this topic see (80)).

With the equations defined, they can be discretized for numerical integration. For the systems considered here, a crucial observation is that simulations must be carried out in full generality. This means that time and spatial variations are equally important, and a disparate range of scales need to be resolved (ranging from at least the size of each compact object, through the scale where gravitational waves are produced, and to the asymptotic region where they are measured). The associated computational cost is quite high, and typical simulations run on hundreds to thousands of processors for hours to weeks, even when efficient resolution of the relevant spatio-temporal scales can be achieved using (for example) adaptive mesh refinement. It is beyond the scope of this review to describe the techniques employed in detail, though we briefly mention them and point to some relevant literature for further details. (See also a few textbooks on

²For a recent review, see (201).

the subject written in recent years (6, 23, 36)).

- Spatial discretization. As far as the gravitational field itself is concerned, solutions are generally smooth (except at singularities) provided smooth initial data are defined because the equations of motions are *linearly degenerate* (i.e. do not induce shocks from smooth initial data). High-order finite difference approximations (e.g. (99)) or spectral decompositions (e.g. (38, 95)) allow for a high degree of accuracy. When matter and the hydrodynamic equations are involved, finite volume methods and high-resolution shock capturing schemes can be used to determine the future evolution of the fluid variables (e.g. (143)).
- Time integration. The method of lines can be straightforwardly implemented once spatial derivatives are computed.
- Constraint enforcement. For systems of interest, several constraints are typically involved. Those coming from Einstein equations themselves are a nonlinear coupled set of PDEs. In general scenarios, these constraints are difficult to enforce directly; instead, a strategy of “constraint damping” is adopted, whereby the equations of motion are modified in a suitable manner via the addition of constraints. The resulting system is thus not different from the initial one when the constraints are satisfied, otherwise the numerical evolution should damp these violations as time progresses. This desirable behavior can be rigorously shown to hold in perturbations off flat spacetime (40, 98) and also “experimentally” verified in simulations involving black holes and neutron stars (e.g. (9, 53, 189, 190)). This technique—whereby the equations are suitably modified to control constraints—has also been extended to other relevant systems of equations. For instance, when considering magnetohydrodynamics or electrodynamics, to control the no-monopole constraint (164, 179).
- Mesh structure, resolution and adaptivity. As mentioned, several different physical scales need to be resolved. For an efficient implementation, techniques like adaptive mesh refinement and multiple patches are in common use (e.g. (26, 67, 72, 139, 141, 205)).
- Parallelization. The equations involved are of hyperbolic type and they lend themselves naturally to a relatively straightforward parallelization. Several computational infrastructures have been developed for numerical relativity purposes, e.g. BAM, Cactus (107) and the Einstein Toolkit (147), Had (108), Whisky, SACRA (15).

3 Brief Description of the Dynamics of a Binary System

Here we review salient properties of the early phase of binary evolution in general relativity to set the stage for subsequent discussion of the nonlinear regime uncovered by numerical simulations. For further details the interested reader can consult (111).

An isolated compact binary evolves due to the emission of gravitational waves, and consequently a bound system will eventually merge. The end state of compact binary mergers (i.e. binary black holes, black hole-neutron star binaries, and all except the least massive binary neutron stars) will be a single Kerr black

hole³. At large separations, in which the local velocity of each object in the binary is small (relative to the speed of light c), a PN expansion (e.g. (32)), where objects are taken as point-particles without internal dynamics, suffices to accurately describe the system. As the orbit shrinks, the faithfulness of such an expansion decreases as velocities become $O(c)$. If either compact object is a neutron star tidal effects may be important; these can be modeled within the PN framework, though again the accuracy of the expansion degrades approaching tidal disruption, which can occur near merger for stellar mass binaries. During this late stage of inspiral full numerical solution must be employed to obtain an accurate description of the dynamics of the geometry and matter. Once a single black hole forms, very shortly afterward (on the order of a few light-crossing times of the Schwarzschild radius) the spacetime can accurately be modeled by black hole perturbation theory, and to a good approximation the matter can be evolved on a stationary black hole background. In the standard jargon of the field the three different stages just described are often referred to as the PN inspiral, nonlinear and “ring-down” stages.

The nonlinear phase can further be subdivided into a late inspiral, plunge and early postmerger epoch. In the first subphase the binary is still in an orbit, though velocities are high, the orbital frequency quickly sweeps upwards, and neutron star tidal dynamics can become relevant (if the companion is a neutron star or black hole with mass $\lesssim 20M_\odot$). The second refers to a rapid increase in the magnitude of the inward radial velocity leading to merger. The plunge is related to the phenomenon of an innermost stable circular orbit (ISCO) of a black hole, and is thus most apparent in a high-mass-ratio compact binary (see e.g. (45, 47)). The last sub-phase begins when either a black hole or a hyper-massive neutron star forms, and lasts while either object is too “distorted” for a straightforward perturbative approach to be applicable. As mentioned above a black hole settles to a stationary state very rapidly, and hence from a computational perspective there is little to gain switching to a perturbative treatment to measure the ring-down waves. By contrast, in certain ranges of parameter space a hyper-massive neutron star can last for several seconds before collapsing to a black hole, which for the full coupled Einstein-matter equations would be too expensive to evolve at present (a rough estimate of the cost is $O(1000)$ CPU hours per ms at “modest” resolution).

3.1 Properties of Gravitational Wave Emission

During the early inspiral stage in which velocities are much smaller than c , to leading order the emission of gravitational waves is proportional to the acceleration of the reduced (trace free) quadrupole moment tensor $Q_{ij}(t)$ of the system (this is textbook material, though for a couple of recent review articles see (44, 79)):

$$h_{ij}^{TT}(t, \vec{x}) = \frac{2G}{rc^4} \frac{\partial^2 Q_{kl}(t-r)}{\partial t^2} \left[\perp^k{}_i \perp^l{}_j - \frac{1}{2} \perp^{kl} \perp_{ij} \right] \quad (1)$$

In the above, h_{ij}^{TT} is the perturbation of the spatial components of the Minkowski metric η_{ij} in the transverse traceless (TT) gauge, written in a Cartesian coordinate system $(t, \vec{x}) = (t, x_i)$. In this gauge there are no space-time or time-time

³Provided cosmic censorship holds, and there are no indications yet that it fails for mergers in four-dimensional, asymptotically flat spacetime.

perturbations of $\eta_{\mu\nu}$, ie $h_{tt}^{TT} = h_{tj}^{TT} = 0$. The center of mass of the source is at the origin, and the above expression assumes the perturbation is measured at a distance $r = |\vec{x}|$ much greater than the characteristic size of the source, here $\sim r_p$, the periaipse of the orbit⁴. The projection tensor $\perp_{ij} = \delta_{ij} - \hat{n}_i \hat{n}_j$, with $\hat{n}_i = x_i/r$, i.e., \hat{n}_i is the unit spatial vector from the source to the observer at location x_i . The above expression is (to leading order) valid in an expanding Universe if the distance r is replaced by the luminosity distance D_l , and time is dilated by a factor $1 + z$, where z is the redshift between the source and the observer.

The projection in (1) encodes the property of general relativity that there are only two linearly independent propagating degrees of freedom, called the cross and plus polarizations. Thus the tensor h_{ij}^{TT} only has two independent non-zero components, which are called h_+ and h_x . To illustrate, ignoring back-reaction, a binary on a circular Keplerian orbit with orbital frequency $\omega = \sqrt{2GM/r_p^3}$ produces a radiation pattern

$$h_+(t, r, \theta, \phi) = \frac{4G}{rc^4} \mathcal{M}^{5/3} (2\omega)^{2/3} \cos(2\omega t + \phi) \left[\frac{1 + \cos^2 \theta}{2} \right], \quad (2)$$

$$h_x(t, r, \theta, \phi) = \frac{4G}{rc^4} \mathcal{M}^{5/3} (2\omega)^{2/3} \sin(2\omega t + \phi) \cos(\theta), \quad (3)$$

with the so-called chirp mass $\mathcal{M} = \eta^{3/5} M$, the symmetric mass ratio $\eta = m_1 m_2 / M^2$, θ is the angle between the observer's line of sight and the axis normal to the plane of the binary, and ϕ is the (arbitrary) initial azimuthal phase.

The above expressions highlight several properties about gravitational emission from compact objects relevant for detection. First, gravitational wave detectors are directly sensitive to the amplitude of the metric perturbation, and not the energy it carries. The former decays as $1/r$, whereas the latter decays as $1/r^2$ (and being proportional to the square of the third time derivative of Q_{ij}), hence an n -fold improvement in the sensitivity of detectors results in an n^3 increase in the observable volume of the Universe. The ‘‘advanced’’ upgrades to the first generation of ground-based interferometric detectors (that will be completed near the end of the decade) are expected to achieve an order-of-magnitude increase in sensitivity over initial LIGO, increasing the range over which binary neutron stars could be observed to hundreds of Mpc, and binary black holes to over a Gpc (1). Note however that these distances assume matched filtering is used to search for signals that would otherwise be buried in detector noise. For this to maximize both detection prospects and parameter extraction requires template waveforms that are phase-accurate to within a fraction of a cycle over the most sensitive band of the detectors (which for adLIGO ranges from ~ 10 Hz to ~ 1 Khz). Over the past two decades this has been the primary goal of the source modeling community; it is being achieved using high-order perturbative methods for the early inspiral, numerical solution for late inspiral and early merger, and perturbations off a single black hole afterward.

Second, the emission is clearly not isotropic. Only plus-polarized waves are radiated along the equator, and the amplitude is half of that radiated along the

⁴We use the periaipse here rather than, say, the semi-major axis, because for highly eccentric systems described later the dominant gravitational wave emission only occurs around periaipse passage. Thus r_p more conveniently characterizes the relevant scale of gravitational wave emission for all eccentricities.

pole orthogonal to the orbit. Thus the distance to which a source can be observed strongly depends on its relative orientation to the detector. Importantly however, this radiation is not strongly beamed and so even non-ideal orientations of the source to the detector can yield detectable signals.

Third, though these expressions only hint at a couple, there are several degeneracies in the signal that could limit accurate extraction of all relevant parameters from a detection. Under radiation reaction the orbit shrinks, and a binary will sweep across a range of frequencies ω , terminating at merger where $\omega_m \approx c^3/GM$. If ω_m is not in band (such as for instance with a binary neutron star merger), at leading order there is essentially complete degeneracy between the chirp mass and the distance to the source. If an electromagnetic counterpart could be observed and a redshift determined, the degeneracy would break. Higher-order effects, in particular if the black holes spin or the masses are unequal, excite higher gravitational wave multipoles that can further lift degeneracies. This demonstrates the need to understand the full details of the gravitational wave emission, and if matter is involved possible electromagnetic counterparts. And as is discussed more throughout this review, such multi-messenger observations could bring us a wealth of information beyond just measuring binary parameters.

3.2 Priors on Binary Parameters

Merger simulations are computationally expensive, taking of order $10^4 - 10^5$ CPU hours for a simulation of the last $O(10)$ orbits of a quasi-circular inspiral of a binary black hole system. This may not sound too extreme, though remember this is just a single point in an eight-dimensional parameter space—mass ratio, six components of the two spin vectors, and eccentricity. The cost goes up with non-vacuum binaries for several reasons. First, in addition to gravity the relevant matter equations (relativistic hydrodynamics at least) need to be solved for. Second, the effective parameter space grows larger. This is in part to characterize unknown physics such as the equation of state (EOS) of matter at nuclear densities, and in part because of new initial conditions, for example a neutron star’s magnetic field configuration. Third, computational fluid dynamics algorithms are typically lower order (to be able to deal with shocks and surfaces) than the high-order finite difference or pseudo-spectral methods used to solve the Einstein equations, hence higher resolution is required for similar accuracy to a comparable vacuum merger.

The preceding discussion highlights that compact object mergers simulations are too demanding to perform a naive, uniform sampling of parameter space to guide the construction of gravitational wave template banks. A promising approach to achieve a more optimal sampling uses the reduced basis method (78), though regardless of the method one can ask what priors can be placed on the range of parameters from either theoretical or observational considerations?

A typical neutron star likely has a mass within the range of ≈ 1 to $2.5 M_\odot$, a radius (which for a given mass is determined by the EOS) in the range ≈ 8 to 15 km, and they are thought to have low spins (see e.g. (133)). For black holes, an obvious theoretical restriction on the spin magnitude is that $|a| \leq 1$. Observations of candidate black holes, assuming general relativity is correct and black holes satisfy the bound, are beginning to provide estimates of spins ranging across all possible magnitudes $|a| \in [0, 1]$ (154, 155). (Allowing for the possibility of naked singularities is not well posed within the framework of classical general relativity,

and without any theoretical/observational guidance perhaps the best one can do with gravitational waves is to seek for inconsistencies from the predictions of general relativity using something akin to the parameterized post-Einsteinian (ppE) approach (238).⁵) Theoretical models suggest the relative orientation of spins are not uniform, either due to properties of the progenitor binary for stellar mass systems, or interactions with surrounding matter or spin-orbit resonant effects during inspiral (35, 86). Nevertheless, neither theory nor observation provides a sufficiently compelling case to dismiss the full range of spins allowed by general relativity. For stellar mass black holes, masses are expected to range from a few to possibly hundreds of solar masses, supermassive black holes lie at least within the range $10^6 - 10^{10} M_{\odot}$, and evidence is mounting for intermediate mass black holes between this range (see e.g. (51, 60, 76, 88, 96, 119, 211)). Consequently, these ranges are sufficiently broad that the mass ratio q is essentially unconstrained, in particular for the closer-to comparable mass binaries that would require full numerical solution.

One parameter that has been argued *can* be constrained, especially for stellar mass binaries, is the orbital eccentricity. The reason for this is that the back-reaction of gravitational wave emission on the orbit tends to reduce eccentricity. To leading order under radiation reaction, the following is a decent approximation to the relationship between periaapse and eccentricity (see (184, 185) for the derivation and full expression)

$$r_p \approx r_{p0} \frac{1 + e_0}{1 + e} \left(\frac{e}{e_0} \right)^{12/19}, \quad (4)$$

where r_{p0}, e_0 are the initial periaapse and eccentricity, respectively. For the moderate initial eccentricities expected when the progenitor of the black hole binary is a stellar binary, $e \sim (r_p/r_{p0})^{19/12}$. Such a binary enters the adLIGO band at $r_p \sim 10^2 \text{ km}$, whereas expected values for r_{p0} are several orders of magnitude larger (see, e.g. (118)), hence e will be completely negligible here. This has focused the majority of work on mergers on the quasi-circular $e = 0$ case. However, there are other mechanisms to form binaries, and some could lead to systems that have high-eccentricity while emitting in the LIGO band. These mechanisms include dynamical capture from gravitational wave emission during a close two-body encounter in a dense cluster (136, 169), a merger induced during a binary-single star interaction in a similar environment (200), and Kozai-resonant enhancement of eccentricity in a hierarchical triple system (11, 13, 129, 210, 231). Event rates are highly uncertain for both classes of binaries (see (1) for a review of quasi-circular inspiral systems, and (68, 124, 136, 169, 225) for discussions of dynamical capture systems), and though quasi-circular inspirals are likely dominant, eccentric mergers may not be completely irrelevant as often assumed in the gravitational wave community. The formation mechanism for supermassive black hole binaries is different (being driven by mergers of the host galaxies of individual black holes), though similarly there are arguments that in some cases non-negligible eccentricity might remain until merger (198).

The difficulty with eccentricity is that it is not “merely” an additional parameter, but changes the qualitative properties of a merger in a manner that challenges both source modeling and data analysis strategies. With regard to

⁵For tests of gravity with electromagnetic signals see e.g. (42).

modeling, the orbital period increases significantly with e for a given r_p , making numerical simulations of multi-orbit mergers very expensive. Perturbative methods have not yet been developed to high order for large eccentricity orbits (though see (31)). Taken together it may be unreasonable to expect templates accurate enough for data analysis using matched filtering any time soon, and different (though sub-optimal) strategies may need to be developed, for example power stacking (68, 220). This implies that for practical purposes there are two “classes” of binaries, quasi-circular inspirals, and large eccentricity, small initial pericenter mergers.

Having discussed broad considerations relevant to the three classes of binaries—black hole-black hole, black hole-neutron star, neutron star-neutron star— we now discuss salient features of each class uncovered through numerical simulations.

4 Binary Black Holes

Due to the “no-hair” property of event horizons in four-dimensional Einstein gravity, isolated single black holes in our Universe are expected to be described almost exactly by the Kerr family of solutions. This is a two-parameter family, labeled by the total gravitational mass M and angular momentum J .⁶ The latter is more conveniently described by a dimensionless spin parameter $a = J/M^2$. As mentioned, an event horizon is only present if $|a| \leq 1$, otherwise the solution exhibits a naked singularity. If such a situation could arise (violating the so-called cosmic censorship conjecture) classical general relativity would not be able to describe the exterior solution nor the dynamics of the object in our Universe. This would offer a prime opportunity to study quantum gravity, though unfortunately to date no theoretical studies of plausible astrophysical processes involving dynamical, strong-field gravity, including gravitational collapse and compact object mergers, have resulted in a naked singularity.⁷

Thus, technical details aside, the study of vacuum binary black hole mergers in general relativity is a well-defined problem characterized by a relatively small set of parameters : the mass ratio q of the binary, the two initial spin vectors \vec{s}_1, \vec{s}_2 of each black hole, the initial eccentricity e_0 and the size of the orbit (parameterized for example by the initial pericenter distance r_{p0}). There is no intrinsic scale in vacuum Einstein gravity, hence there is a trivial map from any solution with a given set of these parameters to a desired total mass M of the binary. In the remainder of this section we present results from the numerical solution of the Einstein field equations for vacuum mergers, discuss some astrophysical consequences, and briefly comment on issues related to testing general relativity from gravitational wave observations of vacuum mergers. For other review articles discussing similar topics see (52, 101, 191).

⁶An isolated black hole can also have a conserved charge, though in astrophysical settings black holes should be neutral to excellent approximation. “Exotic” matter fields could also support additional “hair”, though we do not consider such fields here.

⁷Though see (113) for an intriguing suggestion that near extremal black holes could be “over spun”, and (213), who suggest that collapse of matter with negligible self-pressure and in a highly prolate configuration could lead to naked singularities. It is also well known that naked singularities can arise in spherical collapse of ideal fluids (see e.g. (117)), or critical collapse in a larger class of matter models (see e.g. (97)). However, these examples are either non-generic (whether by imposed symmetries or fine tuning of initial data) or arise in matter that is of arguable relevance to collapse in astrophysical settings (230).

4.1 Results and Applications of Merger Simulations

A couple of important qualitative questions about the merger process have largely been answered. The first relates to cosmic censorship : a broad swath of parameter space has been explored (see for example (105)), and no naked singularities have been found. Furthermore, to the level of scrutiny the solutions have been subjected, the late time behavior is consistent with a spacetime approaching a Kerr solution via quasi-normal mode decay⁸. The second relates to the existence of new “phases” of the merger outside the purview of the perturbative treatments governing the inspiral and ringdown. One line of reasoning argues that owing to the nonlinearity of the field equations, and the fact that the late stages of a merger occur in the most dynamical, strong-field regime of the theory, these new phases would be natural places to expect novel physics. The opposing argument, which turned out to better describe the simulation results, is that the merger is effectively a highly dissipative process that occurs deep within the gravitational potential well of the combined objects, and very little of the spacetime dynamics that occurs there will leave an imprint on the waves radiated outwards. Or stated another way, perturbative methods have been extended to quite high order in v/c in both the conservative and dissipative dynamics of a binary, and black hole perturbation theory begins with an exact strong-field solution; these together capture the “essential” nonlinearities of the problem. As a consequence of this rather smooth behavior a convenient approach to constructing templates is the Effective One Body (EOB) method (46), where re-summed PN inspiral waveforms are smoothly attached to quasi-normal ringdown modes via a transition function calibrated by numerical simulations (for some recent papers see (5, 58, 180)). Most of the work in this regard has been conducted on non-precessing orbits (i.e. any net spin angular momentum is aligned with the orbital angular momentum) or lower-spin black holes, and it remains to be seen how well this technique may work for highly spinning black holes in precessing orbits. See Figure 1 for two examples of gravitational wave emission from merger simulations, and for one of them a match to EOB calculations.

The science gleaned from numerical simulations of vacuum binary mergers has therefore mostly been in details of the process. Important numbers of relevance to astrophysics include the total energy and angular momentum radiated during merger (and consequently the final mass and spin of the remnant black hole), and the recoil, or “kick” velocity of the final black hole to balance net linear momentum radiated. We can not possibly list these numbers for all cases simulated to date (but we do give some citations to relevant literature for further information). Though to give a sense of the physics and order of magnitude of the numbers we highlight a few key results and present some of the simpler fitting formulas.

4.1.1 ENERGY RADIATED. One can think of the energy radiated during a merger coming from two sources : the gravitational binding energy liberated during inspiral, and energy in the geometry of the merger remnant formed during the collision that is emitted as the horizon settles down to its stationary Kerr state (on timescales comparable with the final orbital period). In the extreme-

⁸In theory the quasi-normal ringdown should transition to a power-law decay at very late times. This has been verified for perturbed single black holes. Binary simulations have not yet been carried that far beyond merger, though the motivation for doing so is minimal as the amplitude of these power-law tails is too small to be observable.

mass-ratio limit the former dominates, and the total radiated energy equals the magnitude of the binding energy at the ISCO; for a quasi-circular inspiral this ranges from $\sim 3.8 - 42\%$ of the rest mass of the small black hole depending on the spin of the large black hole; the lower (upper) limit is a retrograde (prograde) equatorial orbit about an extremal Kerr black hole (the Schwarzschild case gives 5.7%). As the mass ratio decreases (i.e. the masses become comparable) the emitted energy increases, and the amount coming from the ringdown grows to a comparable fraction approaching the equal mass limit. Here numerical simulations are required to compute the exact numbers, and it is more useful to quote the value as a percentage of the total gravitational (ADM) energy M (the gravitational mass of the system as measured by an asymptotic observer). A useful formula interpolating between the analytic extreme-mass-ratio limit (top line below) and empirical fits to numerical data (bottom line) was derived by (21) (see (148, 224) for a couple of alternative formulae):

$$\begin{aligned}
 \frac{E_{rad}}{M} \approx & \quad \eta(1 - 4\eta) \left[1 - \tilde{E}_{ISCO}(\tilde{a}) \right] \\
 & + 16\eta^2 [p_0 + 4p_1\tilde{a}(\tilde{a} + 1)].
 \end{aligned} \tag{5}$$

Here $\tilde{a} = \vec{L} \cdot (\vec{S}_1 + \vec{S}_2) / M^2$ is the projection of the sum of the black hole spin vectors onto the orbital angular momentum prior to merger, $p_0 \approx 0.048$, $p_1 \approx 0.017$, and $\tilde{E}_{ISCO}(\tilde{a})$ is the energy of the effective ISCO of the system. This formula fits existing numerical simulation results to within better than a percent in most cases (see (21) for comparisons and more details).

4.1.2 FINAL SPIN. There are numerous formulas characterizing the final spin of the merger remnant that have been constructed via fits to numerical relativity results (for e.g. (22, 224); see also (148) for PN-inspired functions, and (39) for a prescription based on a so-called ‘‘spin expansion’’ that uses symmetry arguments to economize the formulas). Here we give a simple ‘first-principles’ derived expression from (48) that captures the basic physics, and agrees reasonably well with numerical results. The following formula is valid for spins aligned with the orbital angular momentum (see (121), and others cited above for generalizations to precessing binaries):

$$a_f M \approx L_{orb}(r_{ISCO}, a_f) + m_1 a_1 + m_2 a_2. \tag{6}$$

Here $a_f M$ is the spin angular momentum of the remnant (with M approximated by $m_1 + m_2$), $m_1 a_1$ and $m_2 a_2$ are the spin angular momenta of the initial black holes, and $L_{orb}(r_{ISCO}, a_f)$ is the orbital angular momentum of a reduced-mass particle equivalent of the system evaluated at the ISCO of a Kerr black hole using the parameters of the remnant. The interpretation of this is straight-forward : the system radiates angular momentum until the plunge to merger, after which the majority of the remaining spin plus orbital angular momentum is subsumed by the final black hole. Some angular momentum is radiated during ringdown, but this is taken into account in the above formula through the use of the effective ISCO of the remnant black hole. For interest, a quasi-normal mode with frequency ω_m and azimuthal multiple number m has the following relationship between the energy and angular momentum it carries : $J_{rad} \approx (m/\omega_m) E_{rad}$. $m = 2$ is the dominant mode, and for example a Schwarzschild black hole has $\omega_2 \approx 0.38/M$ (27). Though it is not possible to clearly differentiate the quasi-normal part of the wave from

the emission that precedes it, a rough estimate is of order 1–2% of the net energy is emitted in the ringdown for comparable mass mergers.

The formula (6) predicts the final spin to within a few percent in many cases. For example, it gives $a_f/M \approx 0.663$ for the merger of equal-mass, non-spinning black holes; comparing to numerical relativity simulations, an initial estimate was $a_f/M \approx 0.70$ (189), with the latest high-accuracy simulations refining it to $a_f/M \approx 0.6865$ (203).

4.1.3 RECOIL. A recoil in the remnant, namely a velocity post-merger relative to the initial binary center of mass, can arise when there is asymmetric beaming of radiation during the merger. Asymmetry comes from unequal masses and black hole spins. The formulas describing the recoil can be rather involved (see for example (150)), so here we just briefly mention some of the salient features and numbers. Non-spinning binaries with mass ratio q different from unity give rise to a recoil in the plane of the binary, reaching a maximum of $\sim 175\text{km/s}$ (16, 29, 93, 104) for $q \approx 1/5$. Spin introduces additional asymmetry in the radiation by causing the orbital plane to precess and “bob”, which can induce a recoil both in and orthogonal to the plane of the binary. The magnitude of the out-of-plane recoil is sinusoidally modulated by the effectively random initial phase of the binary. Spin can also allow the onset of a plunge to occur at higher frequency, and hence give higher gravitational wave luminosity, which further amplifies the recoil. The bobbing motion (see (191) for an intuitive description of it) is associated with the largest recoils, which remarkably can reach several thousand km/s for appropriately aligned high-magnitude spins (50, 94, 149); see Figure 2 (left panel) for examples.

These largest velocities are well in excess of the escape velocities of even the most massive galaxies. That observational evidence suggests most galaxies harbour central supermassive black holes, together with hierarchical structure formation models of the growth of these galaxies, implies that mergers with very large recoils are rare. If mergers themselves are common, and black holes can have sizable spins as implied by current observations (196), then the typical recoil must be significantly less than the maximum theoretically possible. One possible explanation for this would be if most mergers take place in gas-rich environments, as then torques induced by circumbinary material will tend to align the spins of the black holes with the overall orbital angular momentum, a configuration that has significantly lower maximum recoil (see e.g. (35, 65)). Another, that operates even in vacuum, comes from PN calculations that include spin-orbit coupling, which shows a tendency for the black hole spins to align (anti-align) with each other if the spin of the more massive black hole is initially at least partially aligned (anti-aligned) with the orbital angular momentum (122).

4.1.4 TESTS OF GENERAL RELATIVITY. A further opportunity offered by gravitational wave observations of merging binaries is to test dynamical, strong-field gravity. With obvious caveats associated with our present lack of understanding of dark matter and dark energy, general relativity has so far been shown to provide a consistent description of gravity in all observations and experiments that are constrained by its predictions (see e.g. (233)). Lacking here are tests in the most nonlinear regime of the theory, in particular where black holes can form. Certainly there is no doubt about the existence of massive, dark, ultra compact objects, and observations of (for example) X-ray emission from stellar mass candidates or properties of AGN are consistent with these phenomena being powered

by Kerr black holes. However, that horizon scales cannot be quite resolved at present⁹ together with complexities of the matter physics responsible for the emission prevents precise determination of local properties of the spacetime. Binary black hole mergers, in particular stellar mass systems that are expected to occur largely in vacuum, offer a unique opportunity to study pure, strong-field gravity. General relativity’s ability to predict the entire waveform, which is uniquely determined by a small set of numbers ($M, q, e, \vec{s}_1, \vec{s}_2$ and detector-source orientation parameters) and can consist of hundreds or even thousands of cycles in the LIGO band, can in principle allow for stringent self-consistency tests on high signal-to-noise-ratio (SNR) events.

However there are several issues that complicate this promise to test general relativity in the near future. First, given the lack of events from the initial LIGO observing runs, it is unlikely that adLIGO will observe a very loud event. Hence viable tests may require statistical analysis of a number of low-SNR events, and little work has yet been done to suggest how this might be carried out (see (4) for a recent proposal; related work on constraining the nuclear EOS using multiple mergers events involving neutron stars is also beginning to be investigated—see the discussion in Sec. 5). Second, detection and parameter estimation relies on matched filtering with templates. If the only templates used are those constructed using general relativity, then all information about possible deviations will be projected out¹⁰. If the event has a high SNR, there should be a detectable residual excess power, but again for the typical SNRs expected for adLIGO this is unlikely¹¹. Compounding the problem, despite the large number of proposed alternatives or modifications to general relativity (see for example (232, 233)), almost none have yet been presented that (i) are consistent with general relativity in the regimes where it is well tested, (ii) predict observable deviations in the dynamical strong-field relevant to vacuum mergers, and (iii) possess a classically well-posed initial value problem to be amenable to numerical solution in the strong-field. The notable exceptions are a subset of scalar tensor theories, though these require a time-varying cosmological scalar field for binary black hole systems (109), or one or more neutron stars in the merger (see Sec. 5). Thus there is little guidance on what reasonable strong-field deviations one might expect. Proposed solutions to (at least partially) circumvent these problems include the ppE and related frameworks (4, 238), modified PN waveforms (14), as well as exploiting properties of the uniqueness of Kerr and its quasi-normal mode structure (28, 55).

4.1.5 ECCENTRIC BINARIES. As mentioned above, the majority of the work on binary black hole mergers from the relativity community has focused on quasi-circular inspiral, except for a handful of recent studies (89, 103, 192). One of the interesting results is that so called “zoom-whirl” orbital dynamics is possible for comparable-mass binaries. In the test particle limit, zoom-whirl orbits are

⁹This may change within a few years through VLBA observations of our galaxy’s central black hole, SGA* (41, 43) as well as nearby M87 (64).

¹⁰Note also that it is unlikely that general relativity templates will completely “miss” all events even if there are strong-field deviations. This is because binary pulsar observations confirm the leading order radiative dynamics of general relativity.

¹¹This is not the case for possible space-based detectors, like eLISA, as their exquisite SNR could allow for detecting supermassive binary black holes mergers with masses in the range $10^4 M_\odot < M < 10^7 M_\odot$ out to redshifts of $z \simeq 20$ with a $\text{SNR} \geq 10$. For a recent review see (208).

perturbations of the class of unstable circular geodesics that exist within the ISCO. They exhibit extreme sensitivity to initial conditions, in which sufficiently fine-tuned data can give an arbitrary number of near-circular “whirls” at periapse for a fixed eccentricity. Away from the test particle limit gravitational wave emission adds dissipation to the system; however, what the simulations show is that even in the comparable mass limit the dissipation is not strong enough to eradicate zoom-whirl dynamics, but merely limits how long it can persist. Perhaps the most interesting consequences of high-eccentricity mergers could arise when neutron stars are involved; this is discussed in Sec. 5.

For the vacuum problem, aside from providing information on binary formation channels, high-eccentricity events could in principle offer the most stringent tests of strong-field gravity. The reason is due to the nature of these orbits compared with quasi-circular inspiral: significantly higher velocities are reached at periapses passage, a larger fraction of the total power is radiated in this high v/c regime, and the long time between periapse bursts imply that small deviations in emission could result in large dephasing of the waveform from one burst to the next. However, to date no studies have addressed in any quantitative manner how well general relativity can be constrained using eccentric mergers.

4.2 Further Physics

With the vacuum merger problem essentially under control, the field is now more closely examining the impact a merging black hole binary can have on its astrophysical environment. The most pertinent scenario is a supermassive binary merger, and questions relate to how the rapidly changing gravitational field, ensuing gravitational waves, and possible recoil could perturb surrounding gas, plasma, electromagnetic fields, stars, etc. Here we briefly discuss some of the more interesting and potentially observable phenomena revealed by recent studies.

- *Prompt counterparts to supermassive black hole binaries mergers within circumbinary disks.* First studies of the interaction of binary black holes with surrounding electromagnetic fields and plasma were presented by (176, 177). Though not modeled there, the expected source of these fields and plasma would be a circumbinary disk. More recent work has begun to self-consistently model the disk as well (77, 91). Recall that in the case of a single black hole, the Blandford-Znajek (BZ) mechanism (33) indicates the plasma (coming from an accretion disk) is able to tap rotational energy from the black hole and power an energetic Poynting flux. Tantalizing observational evidence linking the strength of radio signals and black hole spin has been presented by (155). In the context of binary black holes, simulations demonstrated that the spacetime helps stir electromagnetic field lines and that, akin to the BZ mechanism, the plasma is able to tap translational and rotational energy from the system to produce dual jets (176, 177). These jets would act as spacetime tracers, and their behavior can be modeled reasonably well by an extension of the BZ formula. That is, prior to merger, the luminosity from the system obeys $L \simeq B^2 \sum_{i=1,2} [\Omega_H(i)^2 + \kappa v(i)^2]$ where $\Omega_H(i)$, $v(i)$ and κ are the angular rotational velocities of the horizons, the black hole velocities and a relative strength parameter respectively¹². (The value

¹²The dependence on Ω_H acquires higher-order corrections close to maximally spinning cases (223).

of $\kappa \simeq 100$, and indicates that black holes must be moving at $\gtrsim 0.1c$ for a non-trivial contribution unless, of course, they are non-spinning). Notice that unlike the original BZ effect, even if the black holes are non-spinning there could be a sizable luminosity due to the contribution from the translational kinetic energies of the black holes (which can reach $\approx 0.2 - 0.3c$ near merger for quasi-circular inspiral). After merger, a single jet arises with luminosity $L \simeq B^2(\Omega_{H_{final}} + \kappa v_{recoil}^2)$ (though the second term is subleading unless the final black hole has negligible spin, as v_{recoil} is at most $\approx 0.015c$). This behavior implies interesting possibilities for detection of gravitational and electromagnetic waves associated with a merger embedded in a circumbinary disk (see e.g. (161, 170)).

- *Post-merger consequences of binary supermassive black hole mergers.* The merger event can have several interesting consequences due to the large amounts of energy radiated and (for appropriate spins and mass ratios) the recoil of the final black hole; we briefly mention a few here—for recent reviews of this and other astrophysical consequences see (125, 206). With respect to timescales in the disk these effects occur essentially instantaneously. This near-impulsive perturbation of the gravitational potential in the outer parts of the accretion disk could lead to the formation of strong shocks; this, together with subsequent inward migration of the disk, could produce observable electromagnetic emission on timescales of a month to a year afterward (144, 160). The most favored orientations for recoils can produce velocities large enough to significantly displace the remnant from the galactic core, or even eject the black hole from the host galaxy altogether (though as discussed above this is likely quite rare). If the system has a circumbinary accretion disk, the recoil would carry the inner part of the disk with it, and this could be observable in Doppler-displaced emission lines relative to the galactic rest frame (126). Earlier studies have suggested that prior to merger the accretion rate, and hence the luminosity of the nucleus, would be low as the relatively slow migration of the inner edge of the accretion disk decouples from the rapidly shrinking orbit of the binary. Post merger then, AGN-like emission could be reignited once the inner edge of the disk reaches the new ISCO of the remnant black hole. This should be displaced from the galactic center if a large recoil occurred, and could be observable in nearby galaxies (see for example (146)). However, more recent simulations of circumbinary disks using ideal magnetohydrodynamics for the matter shows that complete decoupling does not occur, and relatively high accretion rates can be maintained all the way to merger (34, 77, 166) and afterwards (e.g (212)). The binary orbit in this case causes a modulation in the luminosity of the system, which may be observable. A last effect we mention is that a displaced central black hole should also have its loss-cone refilled, increasing the frequency of close encounters with stars and their subsequent tidal disruption by the black hole, with rates as high as 0.1/yr; the disruption could produce observable electromagnetic emission (219).

- *Binary black hole mergers and galaxy formation.* Galaxy formation models have also been exploited to understanding of the outcome of binary black hole mergers. There is strong stellar, gas-dynamical (127, 128, 153) and electromagnetic (85, 186) evidence for the existence of massive black holes at the centers of galaxies. These central black holes play a fundamental role in our current paradigm of galaxy formation and evolution; for example, they are required to explain quasar and AGN emission (215), as well as cosmic downsizing (37, 56, 202). In the Λ CDM model galaxies merge into increasingly larger ones as cosmic time proceeds, and consequently their massive black holes are expected to merge, ini-

tially via processes such as dynamical friction, with gravitational wave emission only taking over in the very late stages. Results from NR simulations have been utilized to follow the evolution of these black holes through coalescence. More specifically, a number of works studied the mass and spin evolution of super-massive black holes through cosmic time (30, 75, 227, 228), in some cases also accounting for the recoil velocity of the merger remnant (18, 151). It has also been suggested that if a space-based detector such as eLISA becomes available, measurements of the mass ratios of black holes binaries and the precession effects predicted by PN/NR calculations would help to discriminate between competing models of galaxy formation (18, 209).

5 Non-vacuum Binaries

As in the binary black hole case, non-vacuum binaries present a well defined problem, however they need a larger set of parameters to characterize. First, the matter physics introduces a scale, so that unlike the vacuum case the total mass of the system cannot be factored out. Thus the set of parameters needed to describe the orbit are now the masses m_1 and m_2 of the compact objects, their two initial spin vectors \vec{s}_1, \vec{s}_2 (which however is expected to be small for neutron stars), and the initial eccentricity e_0 and size of the orbit (again which we parameterized by the initial pericenter distance r_{p0}). Second, for neutron star matter one must specify the EOS (which for a given mass star determines its radius), and each star's magnetization (strength and dipole direction).

The presence of (magnetized) matter in the system, that is strongly affected by the rapidly varying geometry during coalescence, can naturally induce electromagnetic and neutrino emission in concert with the gravitational waves. A prime example is short Gamma Ray Bursts (sGRBs), and the evidence is mounting that non-vacuum binary mergers provide the central engine for these spectacular astrophysical phenomena (e.g (24, 25, 114, 135, 158, 188, 221)). Thus, in addition to obtaining predictions for the gravitational wave signatures from these events (see Figure 4 for some examples), research using simulations is also focused on gaining a theoretical understanding of their connections to sGRBs, and related phenomena.

Widely separated non-vacuum binaries display the same behavior as binary black holes. Here internal details play a negligible role, as their effects first appear in a Post-Newtonian expansion at order $(v/c)^{10}$. Closer to merger tidal forces introduce subtle deviations at first, growing to quite large deformations at the point of contact in a binary neutron star system, and for a black hole neutron star system can even lead to the disruption of the star prior to merger. For binary neutron stars, if the total mass in the remnant is more than the maximum mass allowed by the EOS, a black hole will eventually form. The intermediate state is called a hypermassive neutron star (HMNS), and is temporarily supported by rotation and thermal pressure. An interesting question then, as illustrated in Figure 4, is how long the HMNS lasts. Once a black hole forms, and following a black hole-neutron star merger, an accretion disk can form. If there is sufficient mass in the disk, this could be the beginning of a jet that would eventually produce a sGRB. A host of other electromagnetic emission is likely as a consequence of these non-vacuum mergers, as is neutrino emission. In the following sections we discuss these in more detail, highlighting the information gained

from numerical relativity simulations. For other review articles in this subject area see (66, 74, 187).

5.1 Binary Neutron Star Mergers

Fully general relativistic studies of binary neutron stars have been an active area of research for over a decade. (For a small sample of recent results in this area see for e.g. (8, 110, 120, 123, 178, 194, 197, 207, 218)). The initial focus of the research was directed toward understanding broad characteristics of the gravitational wave emission, and consequently rather simple treatments of the matter were employed (typically an ideal fluid with polytropic equation of state). These efforts gave a rather robust understanding of the qualitative dynamics of the system, and prepared a solid foundation to increase the realism of the matter modeling in the simulations. In recent years the addition of new physical ingredients have included more realistic equations of state, magnetic fields and plasmas, and some simplistic treatments of neutrino and radiation physics. In this section we review the more interesting developments relevant to astrophysics.

As in the case of binary black holes, several important qualitative questions about the merger process have been elucidated. The first relates to behavior post-merger and, for a sufficiently massive remnant, the onset of collapse to a black hole. A large swath of parameters centered about the observationally favored initial neutron star masses of $\approx 1.4M_{\odot}$, and consistent with the highest-mass neutron stars observed to date ($\approx 2.1M_{\odot}$ see, (12, 62) and related discussion by (133)), show an HMNS forms. From a fundamental gravity point of view, an interesting observation is that this intermediate state can have a highly dense central region, and an effective angular momentum higher than the Kerr bound. Yet, obeying the cosmic censorship conjecture, the object does not evolve to a nakedly singular solution, but is able to efficiently transport angular momentum outward to eventually allow a black hole to form. The black hole settles down to an approximate Kerr solution surrounded by some amount of material in a disk. A crucially important question then is what the timescale for collapse is. This timescale depends sensitively on the initial conditions and several physical properties: the individual neutron star masses and eccentricity of the binary (which influences the initial distribution of mass among the HMNS, bound and ejected material), the EOS, neutrino and photon cooling, and thermal pressure, as well as diverse mechanisms for angular momentum transport. The reason this is such an important question is that the timescale is in principle observable, either directly via the gravitational wave emission (as illustrated in Figure 4, though note that the frequency of the post-merger waves are sufficiently high that the adLIGO detectors will not be sensitive to them except for a highly unlikely nearby event), or indirectly through details of the counterpart electromagnetic/neutrino emission.

Beyond these broad qualitative issues, theoretical studies have been aimed to analyze in detail the coalescence process and characteristics of the gravitational wave emission. As mentioned, early stages of the dynamics are well captured by PN treatments. Approaching merger tidal effects do start to influence the evolution of the orbit, which would be reflected in the gravitational wave emission and could be detected via delicate data analysis (59, 106). Another interesting pre-merger consequence of tidal forces during a quasi-circular inspiral is they can induce resonant oscillations in the interface modes (i-modes) between the

neutron star crust and core that grow large enough to shatter the star’s crust, leading to a potentially observable pre-cursor electromagnetic outburst (226). For highly eccentric close encounters, the tidal force is impulsive in nature. This can similarly shatter the crust (225), and will excite f-mode oscillations in the star (90, 217). The f-modes do emit gravitational waves, though at frequencies that are too high and amplitudes too weak for likely direct detection with adLIGO.

For low eccentricity encounters the stars merge at an orbital frequency that can be estimated by the point at which the stars come into contact, i.e. $\Omega_c \simeq [(m_1 + m_2)(R_1 + R_2)^3]^{1/2}$. At this stage, the stars are traveling at a considerable fraction ($\simeq 10 - 20\%$) of the speed of light, resulting in a violent collision. In the contact region, shock heating is responsible for a considerable amount of mass thrown outwards (some of which becomes unbound) in a rather spheroidal shape. Also, strong shearing in this region induces Kelvin-Helmholtz instabilities and strong differential rotation develops in the newly formed HMNS. The temperature of the HMNS can reach values of $\simeq 30 - 50\text{Mev}$ and, magnetic fields can grow by several orders of magnitude (via winding, tapping kinetic energy and possibly the magneto-rotational instability (MRI), though for this latter process resolutions currently used are still far from that required to adequately resolve it). Tidal tails form during the earlier stages of the merger and distribute material in the vicinity of the equatorial plane. As mentioned, because the total mass of the binary likely exceeds the maximum mass that a stable, non-rotating and cold star might achieve, the subsequent behavior of the HMNS divides into two possible cases: prompt or delayed collapse.

In the prompt collapse case, thermal support and differential rotation are unable to overcome the gravitational attraction and a black hole forms essentially in a free fall time scale. This takes place in binaries with relatively large total mass $M_{tot} \gtrsim 2.6 - 2.8M_\odot$, though the exact value depends intimately on the EOS.

If the collapse does not occur promptly, the post-merger dynamics differs depending on whether the merger involved equal masses or not. In the former case, the newly formed object resembles a dumbbell composed of two cores (the remnants of the individual stars) which gradually turns into an ellipsoidal object as a result of angular momentum transport –primarily via hydrodynamics effects– and angular momentum loss via gravitational waves. For example, Figure 5 illustrates the equatorial density of the remnant following an equal mass binary merger, and another that had $m_1/m_2 = 0.7$. The gravitational waves from a post-merger system has a characteristic frequency in the range $2 \lesssim f \lesssim 4\text{Khz}$, which is proportional (and relatively close) to the Keplerian angular velocity $(M_{HMNS}/R_{HMNS}^3)^{1/2}$ (where M_{HMNS}, R_{HMNS} are the mass and radii of the HMNS, respectively). If the stars have different masses, the stronger tidal forces induced by the more massive star deforms the companion, stripping the outer layers and forming an envelope about the newly formed HMNS. This HMNS now displays two asymmetric cores and behaves as if the more massive core has a satellite that deforms dynamically as time progresses. Regardless of the mass-ratio, a significant amount of material is estimated to lie beyond the ISCO of the black hole that will eventually form, resulting in an accretion disk with mass on the order of $0.01 - 0.3M_\odot$. Typically the more massive disks correlate with longer times to black hole formation, a behavior intuitively expected as there is more time for angular momentum to be transferred outwards to the envelope.

Simulations have also shed light on the processes, and timescales, for such an-

gular momentum transfer. The most important one is hydrodynamical, which begins to operate efficiently after the merger due to the strong torques induced by asymmetries in the HMNS. Other significant mechanisms for this transfer are tied to electromagnetic effects: winding and the MRI can do so by linking the central to outer regions of the HMNS and introducing an effective viscosity in the system. The angular momentum transport timescale due to winding is of the order of $\tau_{wind} \simeq R_{HMNS}/v_A$, with the Alfvén velocity $v_A \simeq B/\sqrt{\rho}$. A few general relativistic simulations have pointed out that the strength of B can increase¹³ from typical premerger values of $10^{10-12}G$, to $10^{15-16}G$ via compression, winding and transfer of hydrodynamical kinetic energy to electromagnetic energy via Kelvin-Helmholtz instabilities (8, 87), which imply timescales $\tau_{wind} \simeq 10-100ms$. We stress however, that present computational resources are still not adequate to give a thorough analysis of this process. For transport driven by the MRI, simulations are even more challenging, so this is still a largely unexplored process within general relativistic simulations of binary neutron star mergers. Nevertheless, estimates indicate $\tau_{MRI} \sim 100ms$ for putative magnetic field strengths of $B \simeq 10^{15}G$. Therefore, either transport mechanism can operate on timescales $\gtrsim 10-100ms$ and aid in expediting the collapse. Cooling via neutrino and radiation transport reduces thermal-pressure support, so it also helps to shorten the time to collapse. However, the timescale for cooling to operate in a significant manner is on the order of seconds. Currently, simulations incorporating both electrodynamics and cooling are actively being pursued and refined.

Beyond the intricate details of the merger and post-merger behavior, there is strong interest in exploring binary neutron star mergers as progenitors of sGRBs and other electromagnetically observable signals. There is already tantalizing observational evidence for the connection between non-vacuum compact binaries mergers and sGRBs (see (24) for a recent review), strengthened by compelling theoretical models that suggest a merger yielding a rapidly accreting black hole could serve as the central energy source through hydrodynamical/plasma or neutrino processes (73, 163). Other models for the origin of at least a class of sGRBs include magnetars produced by binary neutron star mergers, binary white dwarf mergers, or accretion-induced collapse of a white dwarf (142, 159), and the collapse of an accreting neutron star to a black hole (152). Simulations of these systems are providing valuable information to test these models. For instance, once collapse occurs, an initial hyper-accreting stage is observed, followed by a longer fall back accretion phase with the characteristic $t^{-5/3}$ power-law dependence expected from analytic calculations (195). Beyond the burst itself, electromagnetic emission arising from the interaction of ejected material with the ambient medium, or through radioactive decay of r-process elements formed in this material shortly after merger, have been proposed (e.g. (158, 188)). A candidate for this latter “kilonova” event has recently been observed (25, 221). The time scale for this class of emission can be as long as days or weeks following merger, hence it is not amenable to ab initio simulations. However, results from simulations are consistent with properties assumed in these models to give observable signals; in particular, ejected material of order $\lesssim 10^{-4}M_{eject}/M_{\odot} \lesssim 10^{-2}$ traveling with velocities $\simeq 0.1-0.3c$ has been seen in non-eccentric scenarios (with somewhat larger amounts/higher velocities possible in eccentric mergers).

¹³In agreement with analogous results obtained in pseudo-Newtonian (193) or shearing box studies (167).

Finally, a magnetar with magnetic field strength likely in excess of 10^{15}G indeed forms during the merger of magnetized neutron stars, though its lifetime is typically $\lesssim 100\text{ms}$ except for the stiffest of EOS and low-mass binaries (8, 87).

5.1.1 FURTHER PHYSICS We conclude this section with a few miscellaneous topics related to binary neutron star mergers.

- *Magnetosphere interactions.* Neutron stars have among the strongest magnetic fields in the Universe. As in the case of pulsars, they are surrounded by a magnetosphere that arises naturally as argued by (92). It is thus natural to expect that a binary interaction can trigger behavior related to that observed in pulsars (145), though in this case with a tight connection to the orbital dynamics. This has recently been studied by (175, 178), showing that close to the merger event a strong Poynting flux is emitted ($L \simeq 10^{40-43} B_{11}^2 \text{ erg/s}$); see Figure 6 (left panel) for an illustration. As anticipated, many features common to those of pulsars are seen: the existence of gaps in the estimated charge density, shear layers, the development of a current sheet and a striped structure in the toroidal magnetic field. In the binary case however these features bear tight imprints of the binary’s behavior. For instance, as the orbit tightens a ramp-up in Poynting luminosity ensues, and the current sheet structure displays a spiral pattern tied to the orbital evolution of the system. This could provide an important electromagnetic counterpart to the gravitational waves. In addition, the HMNS –which is likely highly magnetized as a result of the collision– can also trigger a strong Poynting flux as it collapses to a black hole (138). The luminosity can be as large as $L \simeq 10^{49} (B/10^{15}\text{G})^2 \text{ erg/s}$, but shuts off abruptly as the black hole forms.
- *Neutrino emissions.* Incipient works are beginning to incorporate estimates of neutrino effects in the system. Since, as mentioned, the typical lifetime of the HMNS would likely be limited to $\lesssim 100\text{ms}$, whereas the timescale for neutrino cooling is in the order of seconds, as a first approximation a full (costly) radiation-transport scheme need not be employed. Instead, a simplified strategy known as a “leakage scheme” (199) has become the starting point. The leakage scheme ignores transport from the diffusion of neutrinos as well as neutrino momentum transfer. What it does model is the possible equilibration of neutrinos, adopts an opaque, hot stellar matter model to describe local neutrino sources and sinks, and accounts for charged-current β processes, electron-positron pair-annihilation and plasmon decays. At low optical depth the scheme uses reaction-rate calculations to estimate the local production and emission of neutrinos. In contrast, at high optical depths it assumes neutrinos are at their equilibrium abundances, and that neutrino/energy losses occur at the diffusion timescale. In between, a suitable interpolation is adopted. Early efforts employing this scheme indicate a binary neutron star merger can produce strong neutrino luminosity of order $\simeq L_\nu \simeq 10^{54} \text{ erg/s}$ (207). Figure 6 (right panel) illustrates the anti-electron neutrino luminosity shortly after an equal-mass ($m_1 = m_2 = 1.5M_\odot$) merger.
- *Eccentric binaries.* Binaries that emit observable gravitational waves while the orbit has high-eccentricity show significant qualitative and quantitative differences in properties of the merger compared with equivalent-mass

quasi-circular inspirals. Because there is more angular momentum in the binary when the two stars collide, typically more mass is stripped off, some fraction of which is ejected and the rest forms an accretion disk (69, 90). This has consequences for the magnitude of ejecta-powered counterparts, abundance of heavy elements produced through r-processes, and the range of initial neutron star masses that can lead to sufficiently massive disks to power an sGRB. The larger rotational energy also implies longer lifetimes for HMNS remnants. As mentioned above, close encounters prior to merger could induce sufficient strain in each NS to shatter its crust, leading to precursor electromagnetic emission (225). Furthermore, f-modes will be excited in each star. This changes the energetics of the orbit and indirectly affect the subsequent gravitational wave emission. The f-modes will also emit gravitational waves directly, though because of their relatively low amplitudes and high frequencies (around 1.5 kHz) they will not be observable with adLIGO-era detectors. Regarding the dominant emission from the orbital motion, as with eccentric binary black hole mergers, the challenge for detection (issues of rates aside) is to construct waveform models accurate enough to use in template-based searches, or devise alternative strategies. Also, even though the integrated energy released is order-of-magnitude comparable to a quasi-circular inspiral, more of it is radiated at higher frequencies in close periaapse, high-eccentricity mergers. For a binary NS this occurs outside adLIGO’s most sensitive range, making such a system unlikely to be detected beyond ≈ 50 Mpc even with matched filtering (68).

- *Alternative gravity theories.* Binary neutron stars are also good candidates to test alternative theories of gravity, in particular those that predict deviations depending upon the coupling of matter to geometry. Scalar-tensor theories posit the existence of a scalar field, that together with geometry, mediates gravitational phenomena. A sub-class of these theories allow a phenomena known as *scalarization*, whereby a sufficiently compact star spontaneously develops a scalar charge that modifies its gravitational interaction with other stars, and allows for dipole radiation from the system (57). Though observations of binary pulsar systems tightly constrain these theories (12), recent numerical work has shown that within the allowable region of parameter space strong departures from general relativity can occur late in the inspiral (19). These differences are triggered close to the merger epoch (yet while the gravitational wave frequencies are still well within the reach of near-future detectors), and significantly modify the dynamics, causing an earlier onset of the plunge (19, 174, 214).

5.2 Black hole–neutron star mergers

The remaining binary that is a target for earth-based gravitational wave detectors is composed of a black hole and a neutron star. Here again, the regime in which the objects are widely separated is well described by a PN approximation, and the binary’s dynamics proceeds as with the other cases discussed above. However, depending on the relation between two key radii—the tidal radius (R_T) and the radius of the ISCO (R_{ISCO})—markedly different behavior is expected near merger. These radii, to leading order, depend on the black hole mass and spin (for R_{ISCO}),

and the binary mass ratio, the star’s mass and EOS (for R_T). Back of the envelope, the tidal radius $R_T \propto R_{NS} (3M_{BH}/M_{NS})^{1/3}$; R_{ISCO} is $6M_{BH}$ for a non-spinning black hole, decreasing (increasing) to M_{BH} ($9M_{BH}$) for a prograde (retrograde) orbit about a maximally spinning Kerr black hole. The importance of these two radii stems from the intuition that a plunge precedes tidal disruption if $R_{ISCO} > R_T$, and the opposite otherwise. This distinction is crucial, as in the former case there would be little difference in the gravitational wave signal compared with a binary black hole merger having the same masses (82). By contrast, if disruption occurs, at its onset gravitational wave emission is sharply suppressed, not only allowing differentiation from the binary black hole case, but also presenting clues about the star’s EOS as this influences the frequency at which the disruption takes place (for a given neutron star mass). It is easy to convince oneself that the disruption possibility favors high spins/comparable masses, while the plunging behavior favors low spins/high mass ratios. Note also that there are fewer channels for electromagnetic emission if disruption does not occur; in particular sGRBs and kilonova require it.

These observations about the nature of black hole/neutron star mergers are clearly born out in simulations. Early studies began with polytropic equations of state and non-spinning black holes, and have since steadily progressed to incorporated more realistic equations of state, now covering a fair range of mass ratios and black hole spins (81, 130, 131). New physics is also being modeled, as we discussed above with binary neutron stars (because, of course, the same code infrastructure can be used for both). Nevertheless, the same caveats concerning neutron star-neutron star binaries apply to black hole-neutron star systems, in that simulations have not yet covered the full range of possible parameters, nor are sufficient computational resources available at present to adequately model all the relevant scales and microphysics.

Regarding the systems in which $R_{ISCO} < R_T$ and disruption occurs, for quasi-circular mergers numerical simulations have found as much as $0.3M_\odot$ of material outside the ISCO following merger (with the largest amounts coming from the low mass ratio/high prograde spin cases). These results have informed fitting formula predicting the amount of diskmass (81), which in turn can be used to estimate the spin of the final black hole (181). Usually a larger fraction of stripped material is bound and subsequently accretes onto the black hole, though as much as $\approx 0.05M_\odot$ can be ejected from the system, moving with speeds $\approx 0.2c$. Typical maximum temperatures following disruption reach $\simeq 80\text{Mev}$. The tail regions are substantially cooler $\simeq 10 - 100\text{Kev}$, though shocks can re-heat this material to $\simeq 1 - 3\text{Mev}$. Interestingly, if the black hole spin and orbital angular momentum direction are misaligned, strong differences arise. For inclinations $\gtrsim 30^\circ$ a very low-mass disk seems capable of forming, with most of the material outside R_{ISCO} and following highly eccentric trajectories having large semi-major axes (81, 130, 131). Based on these trajectories it is estimated this material will return to the black hole to accrete at a rate governed by the familiar law $\dot{M} \propto t^{-5/3}$ (53, 61, 135). Interestingly, the behavior of this material has characteristics consistent with kilonova models. However, the ejecta distribution is mainly around the orbital plane as opposed to the rather spheroidal one arising in binary neutron star mergers. In many cases, the amount of material capable of forming a disk is consistent with estimates for triggering short gamma-ray bursts.

At the other end of the spectrum with low spins and/or high mass ratios in

which $R_T < R_{ISCO}$, the star plunges into the black hole with little or no material left behind. For low-spin black holes this outcome happens for $m_{BH}/m_{NS} \gtrsim 6$; higher spins (or eccentricity, discussed below) can push this to somewhat larger mass ratios. For instance, for $m_{BH} = 10M_\odot, m_{NS} = 1.4M_\odot$, significant disruption only takes place for $a_{BH}/m_{BH} \gtrsim 0.9$ (83). Without disruption electromagnetic and neutrino counterparts such as sGRBs and kilonova are not expected to occur, though as we discuss below there may still be electromagnetic emission if the neutron star has a strong enough magnetic field.

5.2.1 FURTHER PHYSICS. Naturally, as in the binary neutron star case, a plethora of phenomena can be triggered by the system’s dynamics, and diverse works are proceeding to examine these scenarios, several of which we describe here.

- *Magnetized stars.* A few studies have explored the behavior of the system when the neutron star is magnetized. Although electromagnetic effects are too subleading to alter the orbit and gravitational wave emission, the binary’s dynamics can affect properties of the electromagnetic field after merger. In particular, the resulting field topology in the newly formed accretion disk is relevant to assessing whether a jet can be launched from the system. Notice that in the absence of spin-orbit-induced precession near the onset of disruption, the initial poloidal field gets twisted to a mainly toroidal configuration, implying further processes, such as a dynamo/MRI (17), would need to take over to reinstate a poloidal configuration for an efficient jet mechanism to operate (156). The orbit will precess if the black hole is spinning and the spin axis is misaligned with the orbital angular momentum; then the resulting magnetic field topology after disruption has both poloidal and toroidal components. This might aid in giving rise to favorable configurations for jet launching (see the discussion by (81)). Full simulations accurately resolving all of these effects for both precessing and non-precessing configurations have yet to be performed, owing to their heavy computational requirements.
- *Magnetosphere interactions.* As mentioned when discussing black holes interacting with a magnetosphere, the latter is able to tap kinetic energy—rotational or translational—from the black hole if there is a relative motion between them. Such a scenario naturally arises during the inspiral of a magnetized neutron star with a black hole (the binary will not be tidally locked, and so there will be relative motion of the black hole through the magnetic field lines sourced by the neutron star). Basic estimates using a simple “unipolar induction model” indicate the possibility of a strong Poynting luminosity produced by the system (102, 157). First simulations in this direction have recently been completed, obtaining consistent values with $L \simeq 10^{41} B_{12}^2$ (182). Though lacking a detailed account of how this Poynting flux could be converted to observable photons, this offers the possibility of an electromagnetic counterpart preceding the merger.
- *Neutrino emissions.* As in the case of binary neutron stars, simulations are just beginning to incorporate neutrino effects, again using the leakage scheme. Figure 7 shows an example of the neutrino luminosity from one such ongoing investigation, a follow-up study to (61). In this follow-up study they found that the merger of a $1.4M_\odot$ star with a black hole having mass $7M_\odot$ and spin parameter $a/M \equiv J/M^2 = 0.9$ (so significant disruption

tion takes place) yields a peak neutrino luminosity on the order of $\simeq 10^{54}$ erg/s shortly after disruption, decreasing by an order of magnitude after 50ms.

- *Eccentric binaries.* In eccentric black hole-neutron star encounters, similar quantitative and qualitative differences arise compared with quasi-circular inspiral as discussed above for the other systems (possibility of zoom-whirl orbital dynamics, neutron star crust cracking and/or excitation of f-modes during close encounters, typically larger amounts of ejecta and accretion disk mass, etc.). In addition, because the effective ISCO for eccentric orbits of particles orbiting a non-extremal black hole is closer to the event horizon (e.g. for a Schwarzschild black hole the geodesic ISCO moves in from $r = 6M$ to $r = 4M$ going from $e = 0$ to 1), the limit for the onset of observable tidal disruption moves to slightly higher mass ratios¹⁴. Furthermore, in systems where tidal disruption begins outside the ISCO there is the possibility of multiple partial disruptions and accretion episodes prior to the final disruption/merger (71, 217).

6 Gravitational Collapse to a Neutron Star or Black Hole

Considerable efforts have been undertaken to study gravitational collapse to a neutron star or a black hole, in particular within the context of core-collapse supernovae. Here, stars with masses in the range $10M_{\odot} \lesssim M \lesssim 100M_{\odot}$ at zero-age main sequence form cores that can exceed the Chandrasekhar mass and become gravitationally unstable. This leads to collapse that compresses the inner core to nuclear densities, at which point the full consequences of general relativity must be accounted for. Depending upon the mass of the core, it can “bounce” or collapse to a black hole. Figure 8 displays representative snapshots of the behavior of a collapsing $75M_{\odot}$ star at different times. The collapse forms a proto-neutron star that later collapses to a black hole. In the case of a bounce, an outward propagating shock wave is launched that collides with still infalling material and stalls. Observations of core-collapse supernovae imply some mechanism is capable of reviving the shock, which is then able to plow through the stellar envelope and blow up the star. This process is extremely energetic, releasing energies on the order of 10^{53} erg, the majority of which is emitted in neutrinos (for a recent review see (171)). For several decades now, the primary motivation driving theoretical and numerical studies has been to understand what process (or combination of processes) mediates such revival, and how. Several suspects have been identified: heating by neutrinos, (multidimensional) hydrodynamical instabilities, magnetic fields and nuclear burning (see e.g. (49, 115)). With the very disparate time- and space-scales involved, a multitude of physically relevant

¹⁴Note by “observable” tidal disruption we mean disruption that can influence the gravitational waveform and the matter ejected or left to accrete. In theory the location of the event horizon sets the ultimate location for this, though for black hole/neutron star interactions the effective ISCO appears to be a better proxy. The reason is that once a matter parcel crosses the ISCO, barring the rise of strong non-gravitational forces, it will reach the event horizon in of order the light-crossing time of the black hole. Though to date simulations have not included all the relevant matter microphysics, it is unlikely that effects triggered by tidal disruption, e.g. shock heating, shearing of magnetic fields, etc., could grow large enough on such a short time-scale to prevent immediate accretion of the matter.

effects to consider, and the intrinsic cost to accurately model them (e.g. radiation transport is a seven-dimensional problem) progress has been slow. Moreover, electromagnetic observations do not provide much guidance to constrain possible mechanisms as they can not peer deep into the central engine. By contrast, observations of gravitational waves and neutrinos have the potential to do so, provided the exploding star is sufficiently nearby. Thus, in addition to exploring mechanisms capable of reviving the stalled shock, simulations have also concentrated on predicting specific gravitational wave and neutrino signatures. Modeling gravity using full general relativity has only been undertaken recently (173), though prior to this some of the more relevant relativistic effects were incorporated (e.g. (63, 162, 168, 234)). Although the full resolution of the problem is still likely years ahead, interesting insights into fundamental questions and observational prospects have been garnered. For example, simulations have shown that in rotating core-collapse scenarios, gravitational waves can be produced and their characteristics are strongly dependent on properties of the collapse : the precollapse central angular velocity, the development of non-axisymmetric rotational instabilities, postbounce convective overturn, the standing accretion shock instability, protoneutron star pulsations, etc. If a black hole forms, gravitational wave emission is mainly determined by the quasi-normal modes of the newly formed black hole. The typical frequencies of gravitational radiation can lie in the range $\simeq 100 - 1500\text{Hz}$, and so are potential sources for advanced Earth-based gravitational wave detectors (though the amplitudes are sufficiently small that it would need to be a Galactic event). As mentioned, the characteristics of these waveforms depend on the details of the collapse, and, hence, could allow us to distinguish the mechanism inducing the explosion. Neutrino signals have also been calculated, revealing possible correlations between oscillations of gravitational waves and variations in neutrino luminosities. However, current estimates suggest neutrino detections would be difficult for events taking place at kpc distances (173).

7 Further Frontiers

Beyond comparable mass-ratio and comparable radii binaries, NR simulations are starting to explore binaries involving higher mass-ratios or less dense stars: black hole-white dwarf, neutron star-white dwarf, intermediate-mass black holes and main sequence stars, black hole binaries involving intermediate and stellar masses (100), etc. Here, more rapid progress is hampered by the computational cost, as it is considerably higher to simulate the larger range of spatial and temporal scales over which the interesting dynamics takes place. Several approaches have been suggested to address, at least in part, this difficulty. These include the use of implicit-explicit methods to tackle large-mass-ratio binary black holes (134), a suitable re-scaling of physical parameters to model neutron star-white dwarf binaries (183), a “background subtraction” technique to study extreme-mass-ratio systems in which the solution of the dominant gravitational body is known (70), and a reformulation of the problem in terms of a Post-Newtonian approximation incorporating both black hole and matter effects to allow straight-forward modification of existing “Newtonian-based” astrophysical codes (20). These are illustrative examples indicating how the field is progressing beyond traditional boundaries. To date, however, as far as astrophysical

applications are concerned, the predominant focus of NR has been the compact binary problem (and more recently including the study of core-collapse supernovae (173)). Complementary efforts have been directed towards understanding fundamental questions about strongly gravitating settings, some of which have clear astrophysical implications. One example is the question of whether gravitational collapse always leads to a black hole which is described by the Kerr solution, or to a naked singularity. Although most of the cases studied so far have indeed shown the black hole result to be the case, especially in astrophysically relevant contexts, counter examples have been constructed. In $d = 4$ spacetime dimensions these include collapsing matter configurations finely tuned to the threshold of black hole formation (in so-called Type II critical collapse (54), see e.g. (97) for a review and (117) for spherical collapse of ideal fluids.). Due to the fine-tuning required to reach Planck-scale curvatures visible outside an event horizon, it is unlikely critical collapse occurs naturally in the Universe (though see (165) for arguments suggesting it would be relevant if certain primordial black hole formation scenarios occurred). By contrast, this is not the case in higher dimensions in which simulations of a class of black holes (black strings) have shown violations of cosmic censorship can arise generically (140). This not only highlights that Einstein gravity still holds secrets that could be revealed by theoretical studies, but also that surprises of astrophysical significance might be in store if our Universe were in fact higher dimensional.

8 Final Comments

In this review we have described the status of numerical relativity applied in astrophysical contexts. We have focused our presentation on events in which strong gravitational interactions require the full Einstein field equations to unravel all details of the phenomena. Due to page limitations, we have had to choose a representative subset of all relevant activities; nevertheless we hope it is clear that the field has “come of age.” Yet there is still much to learn, and continued efforts will refine numerical relativity’s predictions and application in astrophysics.

9 Acknowledgements

We want to thank our collaborators on work mentioned here: M. Anderson, E. Barausse, W. East, E. Hirschman, S. Liebling, S. McWilliams, P. Motl, D. Neilsen, C. Palenzuela, F. Ramazanoglou, B. Stephens and N. Yunes. We also acknowledge helpful discussions with A. Buonanno, K. Belczynski, E. Berger, D. Brown, C. Fryer, T. Janka, W. Lee, B. Metzger, R. Narayan, E. Poisson, E. Quataert, E. Ramirez-Ruiz, S. Rosswog, A. Spitkovsky and J. Stone. For figures: C. Ott, B. Giacomazzo, F. Foucart, C. Lousto, A. Buonanno, H. Pfeiffer, S. Shapiro, R. Gold, M. Hannam, K. Kyutoku, K. Hotokezaka, M. Shibata. We also thank the participants of the “Chirps, Mergers and Explosions: The Final Moments of Coalescing Compact Binaries” workshop at the Kavli Institute for Theoretical Physics for stimulating discussions. This work was supported in part by an NSERC Discovery Grant and CIFAR (LL), NSF grants PHY-1065710, PHY1305682 and the Simons Foundation(FP). Research at Perimeter Institute is supported by the Government of Canada through Industry Canada and by the Province of Ontario through the Ministry of Research and Innovation.

References

1. J. Abadie et al. TOPICAL REVIEW: Predictions for the rates of compact binary coalescences observable by ground-based gravitational-wave detectors. *Classical and Quantum Gravity*, 27(17):173001, Sept. 2010, 1003.2480.
2. B. P. Abbott et al. LIGO: The Laser Interferometer Gravitational-Wave Observatory. *Rep. Prog. Phys.*, 72:076901, 2009, arXiv:0711.3041 [gr-qc].
3. T. Accadia et al. Status of the Virgo project. *Classical and Quantum Gravity*, 28(11):114002, June 2011.
4. M. Agathos, W. Del Pozzo, T. G. F. Li, C. V. D. Broeck, J. Veitch, et al. TIGER: A data analysis pipeline for testing the strong-field dynamics of general relativity with gravitational wave signals from coalescing compact binaries. 2013, 1311.0420.
5. P. Ajith et al. Inspiral-Merger-Ringdown Waveforms for Black-Hole Binaries with Nonprecessing Spins. *Physical Review Letters*, 106(24):241101, June 2011, 0909.2867.
6. M. Alcubierre. *Introduction to 3+1 Numerical Relativity*. Oxford University Press, 2008.
7. P. Amaro-Seoane, S. Aoudia, S. Babak, P. Binetruy, E. Berti, et al. eLISA: Astrophysics and cosmology in the millihertz regime. 2012, 1201.3621.
8. M. Anderson et al. Magnetized Neutron-Star Mergers and Gravitational-Wave Signals. *Physical Review Letters*, 100(19):191101, May 2008, 0801.4387.
9. M. Anderson, E. W. Hirschmann, L. Lehner, S. L. Liebling, P. M. Motl, D. Neilsen, C. Palenzuela, and J. E. Tohline. Simulating binary neutron stars: Dynamics and gravitational waves. *Phys. Rev. D*, 77(2):024006, 2008, arXiv:0708.2720 [gr-qc].
10. N. Andersson, J. Baker, K. Belczynski, S. Bernuzzi, E. Berti, et al. The Transient Gravitational-Wave Sky. *Class.Quant.Grav.*, 30:193002, 2013, 1305.0816.
11. J. M. Antognini, B. J. Shappee, T. A. Thompson, and P. Amaro-Seoane. Rapid Eccentricity Oscillations and the Mergers of Compact Objects in Hierarchical Triples. 2013, 1308.5682.
12. J. Antoniadis, P. C. C. Freire, N. Wex, T. M. Tauris, R. S. Lynch, M. H. van Kerkwijk, M. Kramer, C. Bassa, V. S. Dhillon, T. Driebe, J. W. T. Hessels, V. M. Kaspi, V. I. Kondratiev, N. Langer, T. R. Marsh, M. A. McLaughlin, T. T. Pennucci, S. M. Ransom, I. H. Stairs, J. van Leeuwen, J. P. W. Verbiest, and D. G. Whelan. A Massive Pulsar in a Compact Relativistic Binary. *Science*, 340:448, Apr. 2013, 1304.6875.
13. F. Antonini, N. Murray, and S. Mikkola. Black hole triple dynamics: implications for gravitational wave detections. 2013, 1308.3674.
14. K. G. Arun, B. R. Iyer, M. S. S. Qusailah, and B. S. Sathyaprakash. Testing post-Newtonian theory with gravitational wave observations. *Class. Quantum Grav.*, 23:L37–L43, 2006, arXiv:gr-qc/0604018.

15. L. Baiotti, M. Shibata, and T. Yamamoto. Binary neutron-star mergers with Whisky and SACRA: First quantitative comparison of results from independent general-relativistic hydrodynamics codes. *Phys.Rev.*, D82:064015, 2010, 1007.1754.
16. J. G. Baker et al. Getting a kick out of numerical relativity. *Astrophys. J.*, 653:L93–L96, 2006, arXiv:astro-ph/0603204.
17. S. A. Balbus and J. F. Hawley. A powerful local shear instability in weakly magnetized disks. 1. linear analysis. 2. nonlinear evolution. *Astrophys. J.*, 376:214–233, 1991.
18. E. Barausse. The evolution of massive black holes and their spins in their galactic hosts. *Mon. Not. R. Astron. Soc.*, 423:2533–2557, July 2012, 1201.5888.
19. E. Barausse et al. Neutron-star mergers in scalar-tensor theories of gravity. *Phys.Rev.*, D87:081506, 2013, 1212.5053.
20. E. Barausse and L. Lehner. A Post-Newtonian approach to black hole-fluid systems. *Phys.Rev.*, D88:024029, 2013, 1306.5564.
21. E. Barausse, V. Morozova, and L. Rezzolla. On the mass radiated by coalescing black-hole binaries. *Astrophys.J.*, 758:63, 2012, 1206.3803.
22. E. Barausse and L. Rezzolla. Predicting the direction of the final spin from the coalescence of two black holes. *Astrophys. J.*, 704:L40–L44, 2009, arXiv:0904.2577 [gr-qc].
23. T. W. Baumgarte and S. L. Shapiro. *Numerical Relativity: Solving Einstein's Equations on the Computer*. June 2010.
24. E. Berger. Short-Duration Gamma-Ray Bursts. 2013, 1311.2603.
25. E. Berger, W. Fong, and R. Chornock. An r-process Kilonova Associated with the Short-hard GRB 130603B. *ApJ. Lett.*, 774:L23, Sept. 2013, 1306.3960.
26. M. J. Berger and J. Olinger. Adaptive mesh refinement for hyperbolic partial differential equations. *J. Comp. Phys.*, 53:484, 1984.
27. E. Berti, V. Cardoso, and A. O. Starinets. Quasinormal modes of black holes and black branes. *Class. Quantum Grav.*, 26:163001, 2009, arXiv:0905.2975 [gr-qc].
28. E. Berti, V. Cardoso, and C. M. Will. Gravitational-wave spectroscopy of massive black holes with the space interferometer LISA. *Phys. Rev. D*, 73:064030, 2006, arXiv:gr-qc/0512160.
29. E. Berti et al. Inspiral, merger, and ringdown of unequal mass black hole binaries: A multipolar analysis. *Phys. Rev. D*, 76:064034, 2007, arXiv:gr-qc/0703053.
30. E. Berti and M. Volonteri. Cosmological Black Hole Spin Evolution by Mergers and Accretion. *Astrophys. J.*, 684:822–828, Sept. 2008, 0802.0025.
31. D. Bini and T. Damour. Gravitational radiation reaction along general orbits in the effective one-body formalism. *Phys.Rev.*, D86:124012, 2012, 1210.2834.

32. L. Blanchet. Gravitational Radiation from Post-Newtonian Sources and Inspiralling Compact Binaries. *Living Rev. Relativity*, 5(3), 2002, arXiv:gr-qc/0202016. <http://www.livingreviews.org/lrr-2002-3>.
33. R. D. Blandford and R. L. Znajek. Electromagnetic extraction of energy from Kerr black holes. *Mon. Not. R. Astron. Soc.*, 179:433–45, 1977.
34. T. Bode, T. Bogdanovic, R. Haas, J. Healy, P. Laguna, and D. M. Shoemaker. Mergers of Supermassive Black Holes in Astrophysical Environments. *Astrophys. J.*, 744:45, 2012, arXiv:1101.4684 [gr-qc].
35. T. Bogdanovic, C. S. Reynolds, and M. C. Miller. Alignment of the spins of supermassive black holes prior to coalescence. *Astrophys. J.*, 661:L147–L150, 2007, arXiv:astro-ph/0703054.
36. C. Bona, C. Bona-Casas, and C. Palenzuela-Luque. Matter Spacetimes. In C. Bona, C. Palenzuela-Luque, and C. Bona-Casas, editors, *Elements of Numerical Relativity and Relativistic Hydrodynamics*, volume 783 of *Lecture Notes in Physics*, Berlin Springer Verlag, page 171, 2009.
37. R. G. Bower, A. J. Benson, R. Malbon, J. C. Helly, C. S. Frenk, C. M. Baugh, S. Cole, and C. G. Lacey. Breaking the hierarchy of galaxy formation. *Mon. Not. R. Astron. Soc.*, 370:645–655, Aug. 2006, astro-ph/0511338.
38. J. P. Boyd. *Chebyshev and Fourier Spectral Methods*. Springer-Verlag, New York, 1989.
39. L. Boyle, M. Kesden, and S. Nissanke. Binary Black-Hole Merger: Symmetry and the Spin Expansion. *Physical Review Letters*, 100(15):151101, Apr. 2008, 0709.0299.
40. O. Brodbeck et al. Einstein’s equations with asymptotically stable constraint propagation. *J. Math. Phys.*, 40:909–923, 1999, arXiv:gr-qc/9809023.
41. A. E. Broderick, V. L. Fish, S. S. Doeleman, and A. Loeb. Constraining the Structure of Sagittarius A*’s Accretion Flow with Millimeter-VLBI Closure Phases. *Astrophys. J.*, 738:38, 2011, 1106.2550.
42. A. E. Broderick, T. Johannsen, A. Loeb, and D. Psaltis. Testing the No-Hair Theorem with Event Horizon Telescope Observations of Sagittarius A*. *ArXiv e-prints*, Nov. 2013, 1311.5564.
43. A. E. Broderick, A. Loeb, and R. Narayan. The Event Horizon of Sagittarius A*. *Astrophys. J.*, 701:1357–1366, 2009, 0903.1105.
44. A. Buonanno. Gravitational waves. 2007, 0709.4682.
45. A. Buonanno, G. B. Cook, and F. Pretorius. Inspiral, merger and ring-down of equal-mass black-hole binaries. *Phys. Rev. D*, 75:124018, 2007, arXiv:gr-qc/0610122.
46. A. Buonanno and T. Damour. Effective one-body approach to general relativistic two-body dynamics. *Phys. Rev. D*, 59:084006, 1999, arXiv:gr-qc/9811091.
47. A. Buonanno, L. E. Kidder, and L. Lehner. Estimating the final spin of a binary black hole coalescence. *Phys. Rev. D*, 77:026004, 2008, arXiv:0709.3839 [astro-ph].
48. A. Buonanno, L. E. Kidder, and L. Lehner. Estimating the final spin of a binary black hole coalescence. *Phys. Rev. D.*, 77(2):026004, Jan. 2008, 0709.3839.

49. A. Burrows et al. Multi-dimensional explorations in supernova theory. *Phys. Rep.*, 442:23–37, 2007, astro-ph/0612460.
50. M. Campanelli et al. Large Merger Recoils and Spin Flips from Generic Black Hole Binaries. *ApJ. Lett.*, 659:L5–L8, Apr. 2007, arXiv:gr-qc/0701164.
51. J. Casares and P. Jonker. Mass Measurements of Stellar and Intermediate Mass Black-Holes. 2013, 1311.5118.
52. J. Centrella et al. The Final Merger of Black-Hole Binaries. *Annual Review of Nuclear and Particle Science*, 60:75–100, Nov. 2010, 1010.2165.
53. S. Chawla et al. Mergers of Magnetized Neutron Stars with Spinning Black Holes: Disruption, Accretion, and fallback. *Phys. Rev. Lett.*, 105:111101, 2010, arXiv:1006.2839 [gr-qc].
54. M. W. Choptuik. Universality and scaling in gravitational collapse of a massless scalar field. *Phys. Rev. Lett.*, 70:9–12, 1993.
55. N. A. Collins and S. A. Hughes. Towards a formalism for mapping the space-times of massive compact objects: Bumpy black holes and their orbits. *Phys. Rev.*, D69:124022, 2004, gr-qc/0402063.
56. D. J. Croton, V. Springel, S. D. M. White, G. De Lucia, C. S. Frenk, L. Gao, A. Jenkins, G. Kauffmann, J. F. Navarro, and N. Yoshida. The many lives of active galactic nuclei: cooling flows, black holes and the luminosities and colours of galaxies. *Mon. Not. R. Astron. Soc.*, 365:11–28, Jan. 2006, astro-ph/0508046.
57. T. Damour and G. Esposito-Farese. Tensor multiscalar theories of gravitation. *Class. Quant. Grav.*, 9:2093–2176, 1992.
58. T. Damour, A. Nagar, and S. Bernuzzi. Improved effective-one-body description of coalescing nonspinning black-hole binaries and its numerical-relativity completion. *Phys. Rev. D.*, 87(8):084035, Apr. 2013, 1212.4357.
59. T. Damour, A. Nagar, and L. Villain. Measurability of the tidal polarizability of neutron stars in late-inspiral gravitational-wave signals. *Phys. Rev.*, D85:123007, 2012, 1203.4352.
60. S. W. Davis, R. Narayan, Y. Zhu, D. Barret, S. A. Farrell, et al. The Cool Accretion Disk in ESO 243-49 HLX-1: Further Evidence of an Intermediate Mass Black Hole. *Astrophys. J.*, 734:111, 2011, 1104.2614.
61. M. B. Deaton, M. D. Duez, F. Foucart, E. O’Connor, C. D. Ott, L. E. Kidder, C. D. Muhlberger, M. A. Scheel, and B. Szilagyi. Black Hole-Neutron Star Mergers with a Hot Nuclear Equation of State: Outflow and Neutrino-cooled Disk for a Low-mass, High-spin Case. *ApJ.*, 776:47, Oct. 2013, 1304.3384.
62. P. B. Demorest, T. Pennucci, S. M. Ransom, M. S. E. Roberts, and J. W. T. Hessels. A two-solar-mass neutron star measured using Shapiro delay. *Nature*, 467:1081–1083, Oct. 2010, 1010.5788.
63. H. Dimmelmeier, J. A. Font, and E. Müller. Relativistic simulations of rotational core collapse. I. Methods, initial models, and code tests. *Astron. Astrophys.*, 388:917–935, 2002, arXiv:astro-ph/0204288.
64. S. S. Doeleman, V. L. Fish, D. E. Schenck, C. Beaudoin, R. Blundell, et al. Jet Launching Structure Resolved Near the Supermassive Black Hole in M87. *Science*, 338:355, 2012, 1210.6132.

65. M. Dotti, M. Volonteri, A. Perego, M. Colpi, M. Ruzskowski, and F. Haardt. Dual black holes in merger remnants II. Spin evolution and gravitational recoil. *Mon. Not. R. Astron. Soc.*, 402:682–690, 2010, arXiv:0910.5729 [astro-ph.HE].
66. M. D. Duez. Numerical relativity confronts compact neutron star binaries: a review and status report. *Class. Quant. Grav.*, 27:114002, 2010, 0912.3529.
67. M. D. Duez, F. Foucart, L. E. Kidder, H. P. Pfeiffer, M. A. Scheel, et al. Evolving black hole-neutron star binaries in general relativity using pseudospectral and finite difference methods. *Phys.Rev.*, D78:104015, 2008, 0809.0002.
68. W. E. East et al. Observing complete gravitational wave signals from dynamical capture binaries. *Phys.Rev.*, D87(4):043004, 2013, 1212.0837.
69. W. E. East and F. Pretorius. Dynamical Capture Binary Neutron Star Mergers. *Astrophys.J.*, 760:L4, 2012, 1208.5279.
70. W. E. East and F. Pretorius. Simulating extreme-mass-ratio systems in full general relativity. *Phys.Rev.*, D87:101502, 2013, 1303.1540.
71. W. E. East, F. Pretorius, and B. C. Stephens. Eccentric black hole-neutron star mergers: Effects of black hole spin and equation of state. *Phys. Rev. D*, 85:124009, Jun 2012.
72. W. E. East, F. Pretorius, and B. C. Stephens. Hydrodynamics in full general relativity with conservative AMR. *Phys.Rev.*, D85:124010, 2012, 1112.3094.
73. D. Eichler, M. Livio, T. Piran, and D. N. Schramm. Nucleosynthesis, neutrino bursts and γ -rays from coalescing neutron stars. *Nature*, 340:126–128, 1989.
74. J. A. Faber and F. A. Rasio. Binary Neutron Star Mergers. *ArXiv e-prints*, Apr. 2012, 1204.3858.
75. N. Fanidakis, C. M. Baugh, A. J. Benson, R. G. Bower, S. Cole, C. Done, and C. S. Frenk. Grand unification of AGN activity in the Λ CDM cosmology. *Mon. Not. R. Astron. Soc.*, 410:53–74, Jan. 2011, 0911.1128.
76. S. Farrell, N. Webb, D. Barret, O. Godet, and J. Rodrigues. An Intermediate-mass Black Hole of Over 500 Solar Masses in the Galaxy ESO 243-49. *Nature*, 460:73–75, 2009, 1001.0567.
77. B. D. Farris et al. Binary Black-Hole Mergers in Magnetized Disks: Simulations in Full General Relativity. *Physical Review Letters*, 109(22):221102, Nov. 2012, 1207.3354.
78. S. E. Field, C. R. Galley, F. Herrmann, E. Oschner, and M. Tiglio. Reduced Basis Catalogs for Gravitational Wave Templates. *Phys. Rev. Lett.*, 106:221102, 2011, arXiv:1101.3765 [gr-qc].
79. E. E. Flanagan and S. A. Hughes. The basics of gravitational wave theory. *New J. Phys.*, 7:204, 2005, arXiv:gr-qc/0501041.
80. J. A. Font. Numerical Hydrodynamics and Magnetohydrodynamics in General Relativity. *Living Reviews in Relativity*, 11:7, Sept. 2008.
81. F. Foucart. Black Hole-Neutron Star Mergers: Disk Mass Predictions. *Phys.Rev.*, D86:124007, 2012, 1207.6304.

82. F. Foucart, L. Buchman, M. D. Duez, M. Grudich, L. E. Kidder, et al. First direct comparison of non-disrupting neutron star-black hole and binary black hole merger simulations. *Phys.Rev.*, D88:064017, 2013, 1307.7685.
83. F. Foucart, M. D. Duez, L. E. Kidder, M. A. Scheel, B. Szilagyi, et al. Black hole-neutron star mergers for 10 solar mass black holes. *Phys.Rev.*, D85:044015, 2012, 1111.1677.
84. D. Garfinkle, W. C. Lim, F. Pretorius, and P. J. Steinhardt. Evolution to a smooth universe in an ekpyrotic contracting phase with $w_{\text{eff}} < -1$. *Phys. Rev. D.*, 78(8):083537, Oct. 2008, 0808.0542.
85. K. Gebhardt, J. Kormendy, L. C. Ho, R. Bender, G. Bower, A. Dressler, S. M. Faber, A. V. Filippenko, R. Green, C. Grillmair, T. R. Lauer, J. Magorrian, J. Pinkney, D. Richstone, and S. Tremaine. Black Hole Mass Estimates from Reverberation Mapping and from Spatially Resolved Kinematics. *Astrophys. J. Lett.*, 543:L5–L8, Nov. 2000, astro-ph/0007123.
86. D. Gerosa, M. Kesden, E. Berti, R. O’Shaughnessy, and U. Sperhake. Resonant-plane locking and spin alignment in stellar-mass black-hole binaries: a diagnostic of compact-binary formation. *Phys.Rev.*, D87:104028, 2013, 1302.4442.
87. B. Giacomazzo, L. Rezzolla, and L. Baiotti. Accurate evolutions of inspiralling and magnetized neutron stars: Equal-mass binaries. *Phys. Rev. D*, 83:044014, 2011, arXiv:1009.2468 [gr-qc].
88. O. Godet, D. Barret, N. Webb, S. Farrell, and N. Gehrels. First evidence for spectral state transitions in the ESO243-49 hyper luminous X-ray source HLX-1. *Astrophys.J.*, 705:L109–L112, 2009, 0909.4458.
89. R. Gold and B. Bruegmann. Eccentric black hole mergers and zoom-whirl behavior from elliptic inspirals to hyperbolic encounters. *Phys.Rev.*, D88:064051, 2013, 1209.4085.
90. R. Gold et al. Eccentric binary neutron star mergers. *Phys.Rev.*, D86:121501, 2012, 1109.5128.
91. R. Gold, V. Paschalidis, Z. B. Etienne, S. L. Shapiro, and H. P. Pfeiffer. Accretion disks around binary black holes of unequal mass: GRMHD simulations near decoupling. *ArXiv e-prints*, Dec. 2013, 1312.0600.
92. P. Goldreich and W. H. Julian. Pulsar electrodynamics. *Astrophys. J.*, 157:869–880, 1969.
93. J. A. González et al. Maximum kick from nonspinning black-hole binary inspiral. *Phys. Rev. Lett.*, 98:091101, 2007, arXiv:gr-qc/0610154.
94. J. A. González et al. Supermassive Recoil Velocities for Binary Black-Hole Mergers with Antialigned Spins. *Physical Review Letters*, 98(23):231101, 2007, arXiv:gr-qc/0702052.
95. P. Grandclement and J. Novak. Spectral methods for numerical relativity. *Living Rev. Relativity*, 12(1), 2009, arXiv:0706.2286 [gr-qc].
96. J. E. Greene and L. C. Ho. Active galactic nuclei with candidate intermediate - mass black holes. *Astrophys.J.*, 610:722–736, 2004, astro-ph/0404110.
97. C. Gundlach. Critical phenomena in gravitational collapse. *Phys.Rept.*, 376:339–405, 2003, gr-qc/0210101.

98. C. Gundlach et al. Constraint damping in the Z4 formulation and harmonic gauge. *Class. Quantum Grav.*, 22:3767–3774, 2005, arXiv:gr-qc/0504114.
99. B. Gustafsson, H.-O. Kreiss, and J. Olinger. *Time dependent problems and difference methods*. Wiley, New York, 1995.
100. R. Haas, R. V. Shcherbakov, T. Bode, and P. Laguna. Tidal Disruptions of White Dwarfs from Ultra-close Encounters with Intermediate-mass Spinning Black Holes. *ApJ.*, 749:117, Apr. 2012, 1201.4389.
101. M. Hannam. Modelling gravitational waves from precessing black-hole binaries: Progress, challenges and prospects. 2013, 1312.3641.
102. B. M. Hansen and M. Lyutikov. Radio and x-ray signatures of merging neutron stars. *Mon.Not.Roy.Astron.Soc.*, 322:695, 2001, astro-ph/0003218.
103. J. Healy, J. Levin, and D. Shoemaker. Zoom-Whirl Orbits in Black Hole Binaries. *Physical Review Letters*, 103(13):131101, Sept. 2009, 0907.0671.
104. F. Herrmann et al. Unequal mass binary black hole plunges and gravitational recoil. *Classical and Quantum Gravity*, 24:33, June 2007, arXiv:gr-qc/0601026.
105. I. Hinder et al. Error-analysis and comparison to analytical models of numerical waveforms produced by the NRAR Collaboration. *Class.Quant.Grav.*, 31:025012, 2013, 1307.5307.
106. T. Hinderer et al. Tidal deformability of neutron stars with realistic equations of state and their gravitational wave signatures in binary inspiral. *Phys. Rev. D*, 81:123016, 2010, arXiv:0911.3535 [astro-ph.HE].
107. CACTUS. home page. <http://www.cactuscode.org>, 2013.
108. HAD. home page. <http://had.liu.edu>, 2013.
109. M. Horbatsch and C. Burgess. Cosmic Black-Hole Hair Growth and Quasar OJ287. *JCAP*, 1205:010, 2012, 1111.4009.
110. K. Hotokezaka et al. Remnant massive neutron stars of binary neutron star mergers: Evolution process and gravitational waveform. *Phys. Rev. D.*, 88(4):044026, 2013, 1307.5888.
111. S. Hughes. Gravitational waves from merging compact binaries. *Ann.Rev.Astron.Astrophys.*, 47:107–157, 2009, 0903.4877.
112. R. N. M. t. IPTA. The International Pulsar Timing Array. *Classical and Quantum Gravity*, 30(22):224010, Nov. 2013.
113. T. Jacobson and T. P. Sotiriou. Over-spinning a black hole with a test body. *Phys.Rev.Lett.*, 103:141101, 2009, 0907.4146.
114. H.-T. Janka, T. Eberl, M. Ruffert, and C. L. Fryer. Black hole-neutron star mergers as central engines of gamma-ray bursts. *Astrophys. J.*, 527:L39–L42, 1999, arXiv:astro-ph/9908290.
115. H.-T. Janka et al. Theory of core-collapse supernovae. *Phys. Rep.*, 442:38–74, Apr. 2007, astro-ph/0612072.
116. M. C. Johnson, H. V. Peiris, and L. Lehner. Determining the outcome of cosmic bubble collisions in full general relativity. *Phys. Rev. D.*, 85(8):083516, Apr. 2012, 1112.4487.
117. P. S. Joshi. Spacetime Singularities. 2013, 1311.0449.

118. V. Kalogera, K. Belczynski, C. Kim, R. W. O’Shaughnessy, and B. Willems. Formation of Double Compact Objects. *Phys.Rept.*, 442:75–108, 2007, astro-ph/0612144.
119. N. Kamizasa, Y. Terashima, and H. Awaki. A New Sample of Candidate Intermediate-Mass Black Holes Selected by X-ray Variability. 2012, 1205.2772.
120. J. D. Kaplan, C. D. Ott, E. P. O’Connor, K. Kiuchi, L. Roberts, and M. Duez. The Influence of Thermal Pressure on Hypermassive Neutron Star Merger Remnants. *ArXiv e-prints*, June 2013, 1306.4034.
121. M. Kesden, G. Lockhart, and E. S. Phinney. Maximum black-hole spin from quasicircular binary mergers. *Phys. Rev. D*, 82:124045, 2010, arXiv:1005.0627 [gr-qc].
122. M. Kesden, U. Sperhake, and E. Berti. Relativistic suppression of black hole recoils. *Astrophys. J.*, 715:1006–1011, 2010, arXiv:1003.4993 [astro-ph.CO].
123. K. Kiuchi, Y. Sekiguchi, K. Kyutoku, and M. Shibata. Gravitational waves, neutrino emissions, and effects of hyperons in binary neutron star mergers. *Class.Quant.Grav.*, 29:124003, 2012, 1206.0509.
124. B. Kocsis and J. Levin. Repeated bursts from relativistic scattering of compact objects in galactic nuclei. *Phys. Rev. D*, 85:123005, Jun 2012.
125. S. Komossa. Recoiling Black Holes: Electromagnetic Signatures, Candidates, and Astrophysical Implications. *Advances in Astronomy*, 2012, 2012, 1202.1977.
126. S. Komossa, H. Zhou, and H. Lu. A recoiling supermassive black hole in the quasar SDSS J092712.65+294344.0. *Astrophys. J.*, 678:L81–L84, 2008, arXiv:0804.4584 [astro-ph].
127. J. Kormendy and L. C. Ho. Coevolution (Or Not) of Supermassive Black Holes and Host Galaxies. *Ann.Rev.Astron.Astrophys.*, 51:511–653, 2013, 1304.7762.
128. J. Kormendy and D. Richstone. Inward Bound—The Search For Supermassive Black Holes In Galactic Nuclei. *Annu. Rev. Astron. Astrophys.*, 33:581, 1995.
129. D. Kushnir, B. Katz, S. Dong, E. Livne, and R. Fernandez. Head-on Collisions of White Dwarfs in Triple Systems Could Explain Type Ia Supernovae. *Astrophys.J.*, 778:L37, 2013, 1303.1180.
130. K. Kyutoku, K. Ioka, and M. Shibata. Ultra-Relativistic Counterparts to Binary Neutron Star Mergers in Every Direction, X-ray-to-Radio Bands and Second-to-Day Timescales. 2012, 1209.5747.
131. K. Kyutoku, K. Ioka, and M. Shibata. Anisotropic mass ejection from black hole-neutron star binaries: Diversity of electromagnetic counterparts. *Phys.Rev.*, D88:041503, 2013, 1305.6309.
132. P. Laguna and D. Garfinkle. Space-time of Supermassive U(1) Gauge Cosmic Strings. *Phys.Rev.*, D40:1011–1016, 1989.
133. J. M. Lattimer and M. Prakash. What a Two Solar Mass Neutron Star Really Means. 2010, 1012.3208.

134. S. R. Lau, G. Lovelace, and H. P. Pfeiffer. Implicit-explicit (IMEX) evolution of single black holes. *Phys.Rev.*, D84:084023, 2011, 1105.3922.
135. W. H. Lee and E. Ramirez-Ruiz. The Progenitors of Short Gamma-Ray Bursts. *New J.Phys.*, 9:17, 2007, astro-ph/0701874.
136. W. H. Lee, E. Ramirez-Ruiz, and G. Van de Ven. Short gamma-ray bursts from dynamically assembled compact binaries in globular clusters: Pathways, rates, hydrodynamics, and cosmological setting. *The Astrophysical Journal*, 720(1):953, 2010.
137. L. Lehner. Numerical relativity: A review. *Class. Quantum Grav.*, 18:R25–R86, 2001, arXiv:gr-qc/0106072.
138. L. Lehner et al. Intense Electromagnetic Outbursts from Collapsing Hypermassive Neutron Stars. *Phys.Rev.*, D86:104035, 2012, 1112.2622.
139. L. Lehner, S. L. Liebling, and O. A. Reula. Amr, stability and higher accuracy. *Class. Quantum Grav.*, 23:S421–S446, 2006, arXiv:gr-qc/0510111.
140. L. Lehner and F. Pretorius. Black Strings, Low Viscosity Fluids, and Violation of Cosmic Censorship. *Phys.Rev.Lett.*, 105:101102, 2010, 1006.5960.
141. L. Lehner, O. Reula, and M. Tiglio. Multi-block simulations in general relativity: High order discretizations, numerical stability, and applications. *Class.Quant.Grav.*, 22:5283–5322, 2005, gr-qc/0507004.
142. A. J. Levan, G. A. Wynn, R. Chapman, M. B. Davies, A. R. King, R. S. Priddey, and N. R. Tanvir. Short gamma-ray bursts in old populations: magnetars from white dwarf-white dwarf mergers. *Mon. Not. R. Astron. Soc.*, 368:L1–L5, May 2006, astro-ph/0601332.
143. R. J. LeVeque. *Numerical Methods for Conservation Laws*. Birkhauser Verlag, Basel, 1992.
144. Z. Lippai, Z. Frei, and Z. Haiman. Prompt shocks in the gas disk around a recoiling supermassive black hole binary. *Astrophys. J.*, 676:L5–L8, 2008, arXiv:0801.0739 [astro-ph].
145. V. M. Lipunov and I. E. Panchenko. Pulsars revived by gravitational waves. *Astron. Astrophys.*, 312:937–940, Aug. 1996, astro-ph/9608155.
146. A. Loeb. Observable Signatures of a Black Hole Ejected by Gravitational-Radiation Recoil in a Galaxy Merger. *Physical Review Letters*, 99(4):041103, July 2007, arXiv:astro-ph/0703722.
147. F. Löffler, J. Faber, E. Bentivegna, T. Bode, P. Diener, R. Haas, I. Hinder, B. C. Mundim, C. D. Ott, E. Schnetter, G. Allen, M. Campanelli, and P. Laguna. The Einstein Toolkit: A Community Computational Infrastructure for Relativistic Astrophysics. *Class. Quantum Grav.*, 29:115001, 2011, arXiv:1111.3344 [gr-qc].
148. C. O. Lousto, M. Campanelli, Y. Zlochower, and H. Nakano. Remnant masses, spins and recoils from the merger of generic black hole binaries. *Classical and Quantum Gravity*, 27(11):114006, June 2010, 0904.3541.
149. C. O. Lousto and Y. Zlochower. Hangup Kicks: Still Larger Recoils by Partial Spin-Orbit Alignment of Black-Hole Binaries. *Phys. Rev. Lett.*, 107:231102, 2011, arXiv:1108.2009 [gr-qc].

150. C. O. Lousto and Y. Zlochower. Modeling maximum astrophysical gravitational recoil velocities. *Phys. Rev. D.*, 83(2):024003, Jan. 2011, 1011.0593.
151. C. O. Lousto, Y. Zlochower, M. Dotti, and M. Volonteri. Gravitational recoil from accretion-aligned black-hole binaries. *Phys. Rev. D*, 85:084015, 2012, arXiv:1201.1923 [gr-qc].
152. A. I. MacFadyen, E. Ramirez-Ruiz, and W. Zhang. X-ray flares following short gamma-ray bursts from shock heating of binary stellar companions. *ArXiv Astrophysics e-prints*, Oct. 2005, astro-ph/0510192.
153. J. Magorrian, S. Tremaine, D. Richstone, R. Bender, G. Bower, A. Dressler, S. M. Faber, K. Gebhardt, R. Green, C. Grillmair, J. Kormendy, and T. Lauer. The Demography of Massive Dark Objects in Galaxy Centers. *Astron. J.*, 115:2285–2305, June 1998, astro-ph/9708072.
154. J. E. McClintock, R. Narayan, S. W. Davis, L. Gou, A. Kulkarni, J. A. Orosz, R. F. Penna, R. A. Remillard, and J. F. Steiner. Measuring the Spins of Accreting Black Holes. *Class. Quantum Grav.*, 28:114009, 2011, arXiv:1101.0811 [astro-ph.HE].
155. J. E. McClintock, R. Narayan, and J. F. Steiner. Black Hole Spin via Continuum Fitting and the Role of Spin in Powering Transient Jets. 2013, 1303.1583.
156. J. C. McKinney and R. D. Blandford. Stability of relativistic jets from rotating, accreting black holes via fully three-dimensional magnetohydrodynamic simulations. *Mon. Not. R. Astron. Soc.*, 394:L126–L130, 2009, arXiv:0812.1060.
157. S. T. McWilliams and J. J. Levin. Electromagnetic extraction of energy from black hole-neutron star binaries. *Astrophys. J.*, 742:90, 2011.
158. B. D. Metzger and E. Berger. What is the Most Promising Electromagnetic Counterpart of a Neutron Star Binary Merger? *ApJ.*, 746:48, Feb. 2012, 1108.6056.
159. B. D. Metzger, E. Quataert, and T. A. Thompson. Short-duration gamma-ray bursts with extended emission from protomagnetar spin-down. *Mon. Not. R. Astron. Soc.*, 385:1455–1460, Apr. 2008, 0712.1233.
160. M. Milosavljević and E. S. Phinney. The afterglow of massive black hole coalescence. *Astrophys. J.*, 622:L93–L96, 2005, arXiv:astro-ph/0410343.
161. P. Mösta, D. Alic, L. Rezzolla, O. Zanotti, and C. Palenzuela. On the detectability of dual jets from binary black holes. *Astrophys. J.*, 749:L32, 2012, arXiv:1109.1177 [gr-qc].
162. B. Müller, H.-T. Janka, and H. Dimmelmeier. A New Multi-dimensional General Relativistic Neutrino Hydrodynamic Code for Core-collapse Supernovae. I. Method and Code Tests in Spherical Symmetry. *Astrophys. J. Supp. Ser.*, 189:104–133, July 2010, 1001.4841.
163. R. Narayan, B. Paczynski, and T. Piran. Gamma-ray bursts as the death throes of massive binary stars. *Astrophys. J.*, 395:L83, 1992, arXiv:astro-ph/9204001.
164. D. Neilsen, E. W. Hirschmann, and R. S. Millward. Relativistic MHD and excision: formulation and initial tests. *Class. Quantum Grav.*, 23:S505, 2006, arXiv:gr-qc/0512147.

165. J. C. Niemeyer and K. Jedamzik. Near-critical gravitational collapse and the initial mass function of primordial black holes. *Phys.Rev.Lett.*, 80:5481–5484, 1998, astro-ph/9709072.
166. S. C. Noble et al. Circumbinary Magnetohydrodynamic Accretion into Inspiral Binary Black Holes. *ApJ.*, 755:51, 2012, 1204.1073.
167. M. Obergaulinger, M. A. Aloy, and E. Müller. Local simulations of the magnetized Kelvin-Helmholtz instability in neutron-star mergers. *Astron. Astrophys.*, 515:A30, June 2010, 1003.6031.
168. M. Obergaulinger et al. Axisymmetric simulations of magnetorotational core collapse: approximate inclusion of general relativistic effects. *Astron.Astrophys.*, 457:209–222, 2006, astro-ph/0602187.
169. R. M. O’Leary, B. Kocsis, and A. Loeb. Gravitational waves from scattering of stellar-mass black holes in galactic nuclei. *Mon. Not. R. Astron. Soc.*, 395:2127–2146, 2009, arXiv:0807.2638 [astro-ph].
170. R. O’Shaughnessy, D. Kaplan, A. Sesana, and A. Kamble. Blindly detecting orbital modulations of jets from merging supermassive black holes. *Astrophys.J.*, 743:136, 2011, 1109.1050.
171. C. D. Ott. The gravitational-wave signature of core-collapse supernovae. *Classical and Quantum Gravity*, 26(6):063001, 2009, 0809.0695.
172. C. D. Ott et al. Dynamics and Gravitational Wave Signature of Collapsar Formation. *Physical Review Letters*, 106(16):161103, 2011, 1012.1853.
173. C. D. Ott et al. General-Relativistic Simulations of Three-Dimensional Core-Collapse Supernovae. *Astrophys.J.*, 768:115, 2013, 1210.6674.
174. C. Palenzuela, E. Barausse, M. Ponce, and L. Lehner. Dynamical scalarization of neutron stars in scalar-tensor gravity theories. 2013, 1310.4481.
175. C. Palenzuela et al. Gravitational and electromagnetic outputs from binary neutron star mergers. *Phys.Rev.Lett.*, 111:061105, 2013, 1301.7074.
176. C. Palenzuela, T. Garrett, L. Lehner, , and S. L. Liebling. Magnetospheres of black hole systems in force-free plasma. *Phys. Rev. D*, 82:044045, 2010, arXiv:1007.1198 [gr-qc].
177. C. Palenzuela, L. Lehner, and S. L. Liebling. Dual jets from binary black holes. *Science*, 329:927–930, 2010, arXiv:1005.1067 [astro-ph.HE].
178. C. Palenzuela, L. Lehner, S. L. Liebling, M. Ponce, M. Anderson, et al. Linking electromagnetic and gravitational radiation in coalescing binary neutron stars. *Phys.Rev.*, D88:043011, 2013, 1307.7372.
179. C. Palenzuela, L. Lehner, and S. Yoshida. Understanding possible electromagnetic counterparts to loud gravitational wave events: Binary black hole effects on electromagnetic fields. *Phys. Rev. D*, 81:084007, 2010, arXiv:0911.3889 [gr-qc].
180. Y. Pan et al. Inspiral-merger-ringdown waveforms of spinning, precessing black-hole binaries in the effective-one-body formalism. 2013, 1307.6232. [arXiv:1307.6232].
181. F. Pannarale. Black hole remnant of black hole-neutron star coalescing binaries with arbitrary black hole spin. 2013, 1311.5931.

182. V. Paschalidis, Z. B. Etienne, and S. L. Shapiro. General relativistic simulations of binary black hole-neutron stars: Precursor electromagnetic signals. *Phys.Rev.*, D88:021504, 2013, 1304.1805.
183. V. Paschalidis, Y. T. Liu, Z. Etienne, and S. L. Shapiro. The merger of binary white dwarf–neutron stars: Simulations in full general relativity. *Phys.Rev.*, D84:104032, 2011, 1109.5177.
184. P. C. Peters. Gravitational radiation and the motion of two point masses. *Phys. Rev.*, 136:B1224–B1232, 1964.
185. P. C. Peters and J. Mathews. Gravitational radiation from point masses in a Keplerian orbit. *Phys. Rev.*, 131:435–440, 1963.
186. B. M. Peterson, L. Ferrarese, K. M. Gilbert, S. Kaspi, M. A. Malkan, D. Maoz, D. Merritt, H. Netzer, C. A. Onken, R. W. Pogge, M. Vestergaard, and A. Wandel. Central Masses and Broad-Line Region Sizes of Active Galactic Nuclei. II. A Homogeneous Analysis of a Large Reverberation-Mapping Database. *Astrophys. J.*, 613:682–699, Oct. 2004, astro-ph/0407299.
187. H. P. Pfeiffer. Numerical simulations of compact object binaries. *Class.Quant.Grav.*, 29:124004, 2012, 1203.5166.
188. T. Piran, E. Nakar, and S. Rosswog. The electromagnetic signals of compact binary mergers. *Mon. Not. R. Astron. Soc.*, 430:2121–2136, Apr. 2013, 1204.6242.
189. F. Pretorius. Evolution of binary black-hole spacetimes. *Phys. Rev. Lett.*, 95:121101, 2005, arXiv:gr-qc/0507014.
190. F. Pretorius. Simulation of binary black hole spacetimes with a harmonic evolution scheme. *Class. Quantum Grav.*, 23:S529–S552, 2006, arXiv:gr-qc/0602115.
191. F. Pretorius. Binary black hole coalescence. In M. Colpi, P. Casella, V. Gorini, U. Moschella, and A. Possenti, editors, *Physics of Relativistic Objects in Compact Binaries: from Birth to Coalescence*, pages 305–369. Springer, Heidelberg, Germany, 2009, arXiv:0710.1338 [gr-qc].
192. F. Pretorius and D. Khurana. Black hole mergers and unstable circular orbits. *Class. Quantum Grav.*, 24:S83–S108, 2007, arXiv:gr-qc/0702084.
193. D. J. Price and S. Rosswog. Producing Ultrastrong Magnetic Fields in Neutron Star Mergers. *Science*, 312:719–722, May 2006, astro-ph/0603845.
194. J. S. Read et al. Matter effects on binary neutron star waveforms. *Phys.Rev.*, D88:044042, 2013, 1306.4065.
195. M. J. Rees. Tidal disruption of stars by black holes of 10 to the 6th-10 to the 8th solar masses in nearby galaxies. *Nature*, 333:523–528, June 1988.
196. C. S. Reynolds. The Spin of Supermassive Black Holes. *Class.Quant.Grav.*, 30:244004, 2013, 1307.3246.
197. L. Rezzolla et al. Accurate evolutions of unequal-mass neutron-star binaries: properties of the torus and short GRB engines. *Class. Quantum Grav.*, 27:114105, 2010, arXiv:1001.3074 [gr-qc].
198. C. Roedig and A. Sesana. Origin and Implications of high eccentricities in massive black hole binaries at sub-pc scales. *J.Phys.Conf.Ser.*, 363:012035, 2012, 1111.3742.

199. M. Ruffert, H.-T. Janka, K. Takahashi, and G. Schäfer. Coalescing neutron stars – a step towards physical models, ii. neutrino emission, neutron tori, and gamma-ray bursts. *Astron. Astrophys.*, 319:122–153, 1997, arXiv:astro-ph/9606181.
200. J. Samsing, M. MacLeod, and E. Ramirez-Ruiz. The Formation of Eccentric Compact Binary Inspirals and the Role of Gravitational Wave Emission in Binary-Single Stellar Encounters. 2013, 1308.2964.
201. O. Sarbach and M. Tiglio. Continuum and Discrete Initial-Boundary-Value Problems and Einstein’s Field Equations. *Living Rev.Rel.*, 15:9, 2012, 1203.6443.
202. E. Scannapieco, J. Silk, and R. Bouwens. AGN Feedback Causes Downsizing. *Astrophys. J. Lett.*, 635:L13–L16, Dec. 2005, astro-ph/0511116.
203. M. A. Scheel, M. Boyle, T. Chu, L. E. Kidder, K. D. Matthews, and H. P. Pfeiffer. High-accuracy waveforms for binary black hole inspiral, merger, and ringdown. *Phys. Rev. D*, 79:024003, 2009, arXiv:0810.1767 [gr-qc].
204. P. Schmidt et al. Tracking the precession of compact binaries from their gravitational-wave signal. *Phys. Rev. D*, 84:024046, 2011, arXiv:1012.2879 [gr-qc].
205. E. Schnetter, S. H. Hawley, and I. Hawke. Evolutions in 3D numerical relativity using fixed mesh refinement. *Class. Quantum Grav.*, 21:1465–1488, 2004, arXiv:gr-qc/0310042.
206. J. D. Schnittman. Astrophysics of Super-massive Black Hole Mergers. *Class.Quant.Grav.*, 30:244007, 2013, 1307.3542.
207. Y. Sekiguchi et al. Gravitational waves and neutrino emission from the merger of binary neutron stars. *Phys.Rev.Lett.*, 107:051102, 2011, 1105.2125.
208. P. A. Seoane et al. The Gravitational Universe. 2013, 1305.5720.
209. A. Sesana, J. Gair, E. Berti, and M. Volonteri. Reconstructing the massive black hole cosmic history through gravitational waves. *Phys. Rev. D*, 83:044036, 2011, arXiv:1011.5893 [astro-ph].
210. N. Seto. Highly Eccentric Kozai Mechanism and Gravitational-Wave Observation for Neutron Star Binaries. *Phys.Rev.Lett.*, 111:061106, 2013, 1304.5151.
211. F. Shankar. The Demography of Super-Massive Black Holes: Growing Monsters at the Heart of Galaxies. *New Astron.Rev.*, 53:57–77, 2009, 0907.5213.
212. S. L. Shapiro. Filling the disk hollow following binary black hole merger: The transient accretion afterglow. *Phys.Rev.*, D81:024019, 2010, 0912.2345.
213. S. L. Shapiro and S. A. Teukolsky. Formation of naked singularities: The violation of cosmic censorship. *Phys. Rev. Lett.*, 66:994–997, 1991.
214. M. Shibata, K. Taniguchi, H. Okawa, and A. Buonanno. Coalescence of binary neutron stars in a scalar-tensor theory of gravity. 2013, 1310.0627.
215. A. Soltan. Masses of quasars. *Mon. Not. R. Astron. Soc.*, 200:115–122, July 1982.
216. K. Somiya. Detector configuration of KAGRA: The Japanese cryogenic gravitational-wave detector. *Class.Quant.Grav.*, 29:124007, 2012, 1111.7185.

217. B. C. Stephens, W. E. East, and F. Pretorius. Eccentric Black Hole-Neutron Star Mergers. *Astrophys. J. Lett.*, 737(1):L5, 2011, 1105.3175.
218. B. C. Stephens, S. L. Shapiro, and Y. T. Liu. Collapse of magnetized hypermassive neutron stars in general relativity: Disk evolution and outflows. *Phys.Rev.*, D77:044001, 2008, 0802.0200.
219. N. Stone and A. Loeb. Prompt tidal disruption of stars as an electromagnetic signature of supermassive black hole coalescence. *Mon. Not. R. Astron. Soc.*, 412:75–80, 2011, 1004.4833.
220. K. S. Tai, S. T. McWilliams, and F. Pretorius. Detecting gravitational waves from highly eccentric compact binaries. 2014, 1403.7754.
221. N. R. Tanvir et al. A ‘kilonova’ associated with the short-duration γ -ray burst GRB130603B. *Nature*, 500:547–549, 2013, 1306.4971.
222. A. Taracchini, A. Buonanno, Y. Pan, T. Hinderer, M. Boyle, et al. Effective-one-body model for black-hole binaries with generic mass ratios and spins. 2013, 1311.2544.
223. A. Tchekhovskoy, R. Narayan, and J. C. McKinney. Black Hole Spin and The Radio Loud/Quiet Dichotomy of Active Galactic Nuclei. *ApJ.*, 711:50–63, Mar. 2010, 0911.2228.
224. W. Tichy and P. Marronetti. Final mass and spin of black-hole mergers. *Phys. Rev. D.*, 78(8):081501, Oct. 2008, 0807.2985.
225. D. Tsang. Shattering Flares During Close Encounters of Neutron Stars. *Astrophys.J.*, 777:103, 2013, 1307.3554.
226. D. Tsang et al. Resonant Shattering of Neutron Star Crusts. *Phys.Rev.Lett.*, 108:011102, 2012, 1110.0467.
227. M. Volonteri, M. Sikora, and J.-P. Lasota. Black Hole Spin and Galactic Morphology. *Astrophys. J.*, 667:704–713, Oct. 2007, 0706.3900.
228. M. Volonteri, M. Sikora, J.-P. Lasota, and A. Merloni. The Evolution of Active Galactic Nuclei and their Spins. *Astrophys. J.*, 775:94, Oct. 2013, 1210.1025.
229. C. L. Wainwright et al. Simulating the universe(s): from cosmic bubble collisions to cosmological observables with numerical relativity. 2013, 1312.1357. [arXiv:1312.1357].
230. R. M. Wald. Gravitational Collapse and Cosmic Censorship. *ArXiv General Relativity and Quantum Cosmology e-prints*, Oct. 1997, gr-qc/9710068.
231. L. Wen. On the Eccentricity Distribution of Coalescing Black Hole Binaries Driven by the Kozai Mechanism in Globular Clusters. *Astrophys. J.*, 598:419–430, 2003, astro-ph/0211492.
232. C. M. Will. *Theory and Experiment in Gravitational Physics*. Mar. 1993.
233. C. M. Will. The confrontation between general relativity and experiment. *Living Rev. Relativity*, 9(3), 2006, arXiv:gr-qc/0510072. <http://www.livingreviews.org/lrr-2006-3>.
234. A. Wongwathanarat, H.-T. Janka, and E. Mueller. Three-dimensional neutrino-driven supernovae: Neutron star kicks, spins, and asymmetric ejection of nucleosynthesis products. *AA 552.*, A126, 2013, 1210.8148.

235. B. Xue, D. Garfinkle, F. Pretorius, and P. J. Steinhardt. Nonperturbative analysis of the evolution of cosmological perturbations through a nonsingular bounce. *Phys. Rev. D.*, 88(8):083509, Oct. 2013, 1308.3044.
236. C.-M. Yoo and H. Okawa. Black Hole Universe with Λ . *ArXiv e-prints*, Apr. 2014, 1404.1435.
237. C.-M. Yoo, H. Okawa, and K.-i. Nakao. Black-Hole Universe: Time Evolution. *Physical Review Letters*, 111(16):161102, Oct. 2013, 1306.1389.
238. N. Yunes and F. Pretorius. Fundamental theoretical bias in gravitational wave astrophysics and the parametrized post-Einsteinian framework. *Phys. Rev. D*, 80:122003, 2009, arXiv:0909.3328 [gr-qc].
239. X. Zhao and G. J. Mathews. Effects of structure formation on the expansion rate of the universe: an estimate from numerical simulations. *Phys.Rev.*, D83:023524, 2011, 0912.4750.

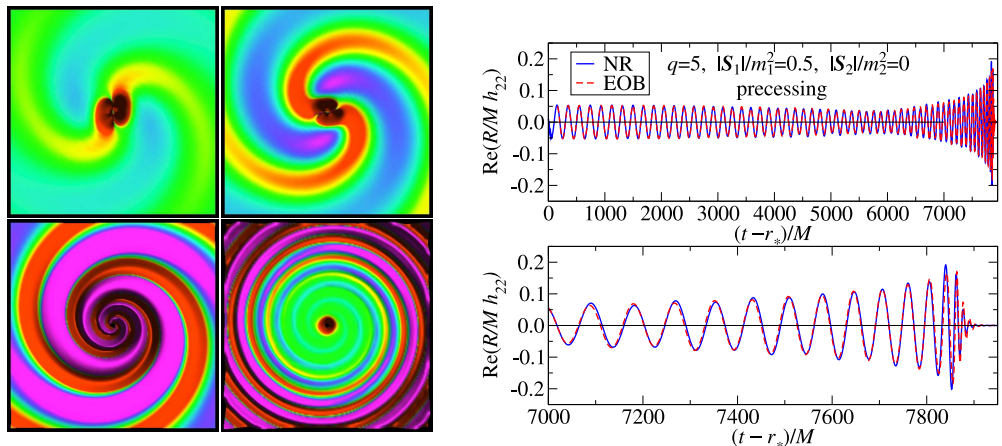


Figure 1: (left) A depiction of the gravitational waves emitted during the merger of two equal-mass (approximately) nonspinning black holes, from (45). Shown is a color-map of the real component of the Newman-Penrose scalar Ψ_4 multiplied by r along a slice through the orbital plane, which far from the black holes is proportional to the second time derivative of the plus polarization (green is 0, toward violet (red) positive (negative)). The top left and right panels show the dominantly quadrupolar inspiral waves $\sim 150M$ and $\sim 75M$ before merger respectively. The bottom left panel is near the peak of the wave emission at merger, and bottom right shows the ringdown waves propagating out $\sim 75M$ after merger. The size of each box is around $100M^2$. (right) Gravitational wave emission measured from a numerical relativity simulation of a binary black hole merger (NR) overlaid with an NR-calibrated effective one body calculation (EOB), from (222). The binary has a mass ratio $q = 5$, the more massive black hole has a dimensionless spin of $a = 0.5$ with direction of the spin axis initially in the plane of the orbit, and the second less-massive black hole is non-rotating. That the amplitude of the wave is not monotonically increasing during inspiral is a manifestation of the modulation induced by precession of the orbital plane.

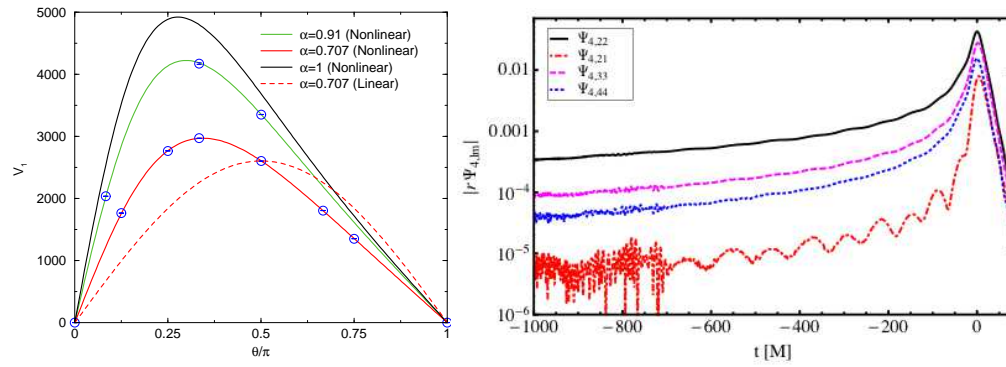


Figure 2: (left) Recoil velocities from equal mass, spinning binary black hole merger simulations (circles) together with analytical fitting functions. Each black hole has the same spin magnitude α , equal but opposite components of the spin vector within the orbital plane, and θ is the initial angle between each spin vector and the orbital angular momentum. The dashed line corresponds to a fitting formula that depends linearly on the spins, whereas solid lines add nonlinear spin contributions. (from (149)). (right) Strength of different modes in the gravitational waves from a binary black hole merger with mass ratio $M_1/M_2 = 3$, and spins $a_1 = 0.75, a_2 = 0$. This system exhibits a marked precession that complicates the multipolar mode structure seen in a fixed observer’s frame. However, a transformation to a co-precessing “quadrupole aligned” frame, as shown in this figure, illustrates that the main radiation channel is still the $l = 2, m = 2$ mode (from (204)).

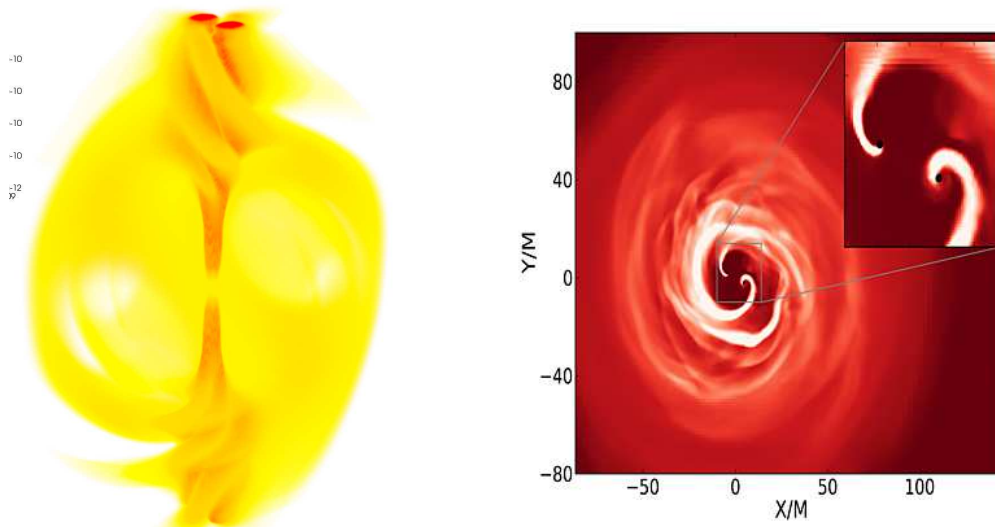


Figure 3: (left) Poynting flux produced by the interaction of an orbiting black hole binary with a surrounding magnetosphere. The “braided” jet structure is induced by the orbital motion of the black holes (from (177)). (right) Rest-mass density induced by a supermassive black hole binary interacting with a magnetized disk prior to when the binary “decouples” from the disk, namely when the gravitational wave backreaction timescale becomes smaller than the viscous timescale (from (77)).

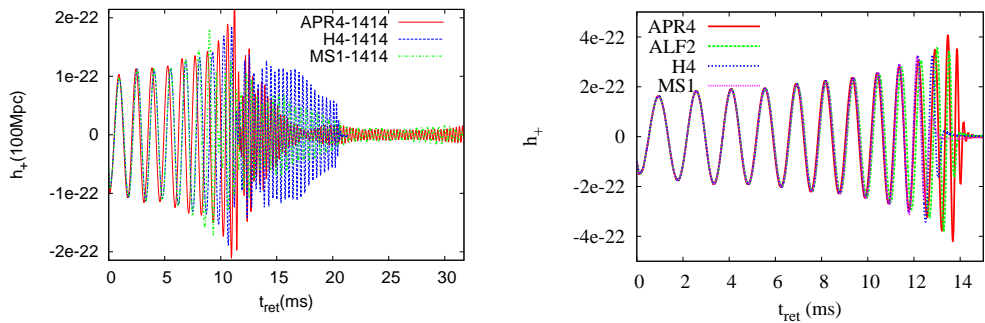


Figure 4: Examples of the “plus” polarization component of gravitational waves from binary neutron star mergers, measured 100 Mpc from the source along the direction of the orbital angular momentum. The different curves correspond to different choices of the equations of state (EOS) of the neutron star matter, labeled APR4, ALF2, H4 and MS1. For a $1.4M_{\odot}$ neutron star, the APR4, ALF2, H4, MS1 EOS give radii of 11.1, 12.4, 13.6, 14.4 km respectively. (left) Mergers of an equal mass binary neutron star system (with $m_1 = m_2 = 1.4M_{\odot}$). A hypermassive neutron star (HMNS) is formed at merger, but how long it survives before collapsing to a black hole strongly depends on the EOS. The H4 case collapses to a black hole ≈ 10 ms after merger; the APR4 and MS1 cases have not yet collapsed ≈ 35 ms after merger when the simulations were stopped (the MS1 EOS allows a maximum total mass of $2.8M_{\odot}$, so this remnant may be stable). The striking difference in gravitational wave signatures is self-evident (from (110)). (right) Emission from black hole-neutron star mergers, with $m_{BH} = 4.05M_{\odot}$, $m_{NS} = 1.35M_{\odot}$. Variation with EOS is primarily due to coalescence taking place earlier for larger radii neutron stars (from (131)).

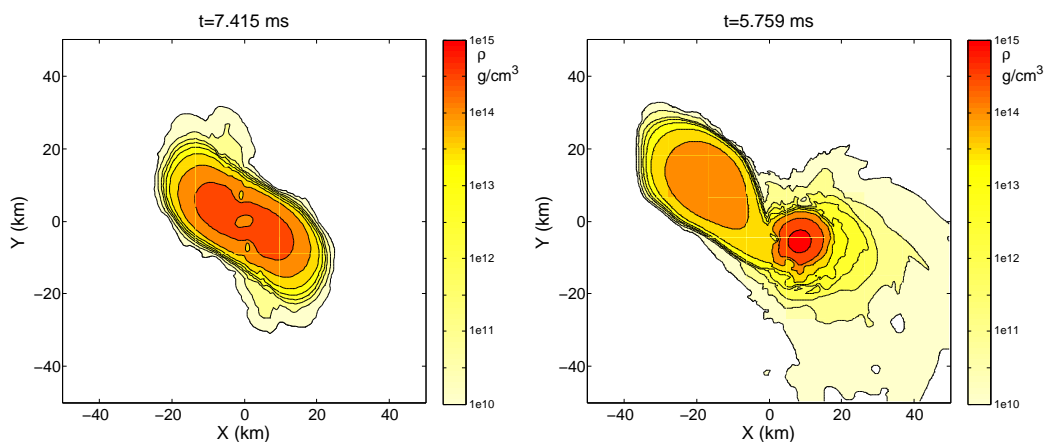


Figure 5: Equatorial density profiles ≈ 3 ms after merger from an equal (left) and unequal (right) mass binary neutron star system. The left panel corresponds to a system with $m_1 = m_2 = 1.643M_{\odot}$ baryonic mass. The right panel corresponds to $m_1 = 1.304$, $m_2 = 1.805M_{\odot}$ baryonic masses (from (197)).

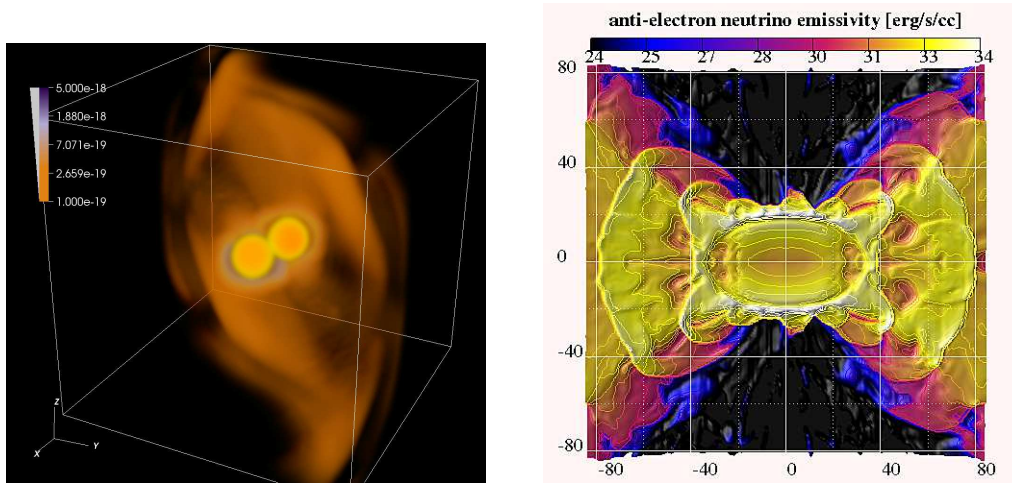


Figure 6: (left) Poynting flux produced by the magnetospheric interaction of orbiting, magnetized (with $B = 10^{12}\text{G}$), equal-mass ($m_1 = m_2 = 1.4M_\odot$) neutron stars $\simeq 1.5\text{ms}$ before merger (from (175)). (right) Anti-electron neutrino luminosity in the $x - z$ plane, 15ms after an equal mass ($m_1 = m_2 = 1.5M_\odot$) binary neutron star merger (from (207)).

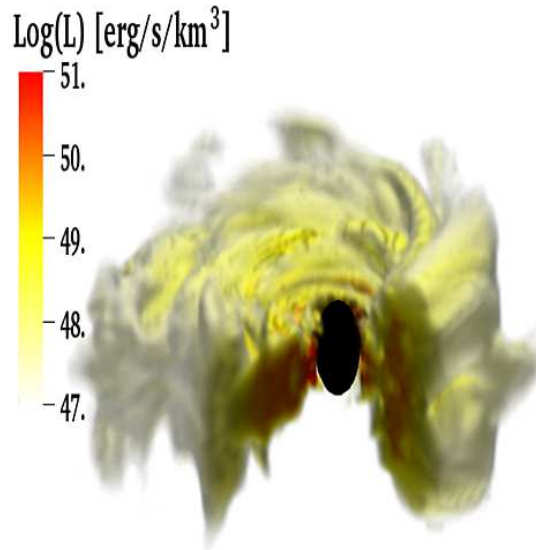


Figure 7: Luminosity from all neutrino species at $\simeq 12.5\text{ms}$ after the merger of a black hole ($M_{BH} = 7M_\odot$) with a neutron star ($M_{NS} = 1.4M_\odot$, described by the “LS220” equation of state). The emission region coincides roughly with the disk; namely densities $\rho > 3 \times 10^9 \text{g/cm}^3$ are approximately within the white region, $\rho > 2 \cdot 10^{10} \text{g/cm}^3$ the red/orange regions, and the maximum density in the disk is $\simeq 6 \cdot 10^{11} \text{g/cm}^3$. (Figure from F. Foucart for the SXS Collaboration.)

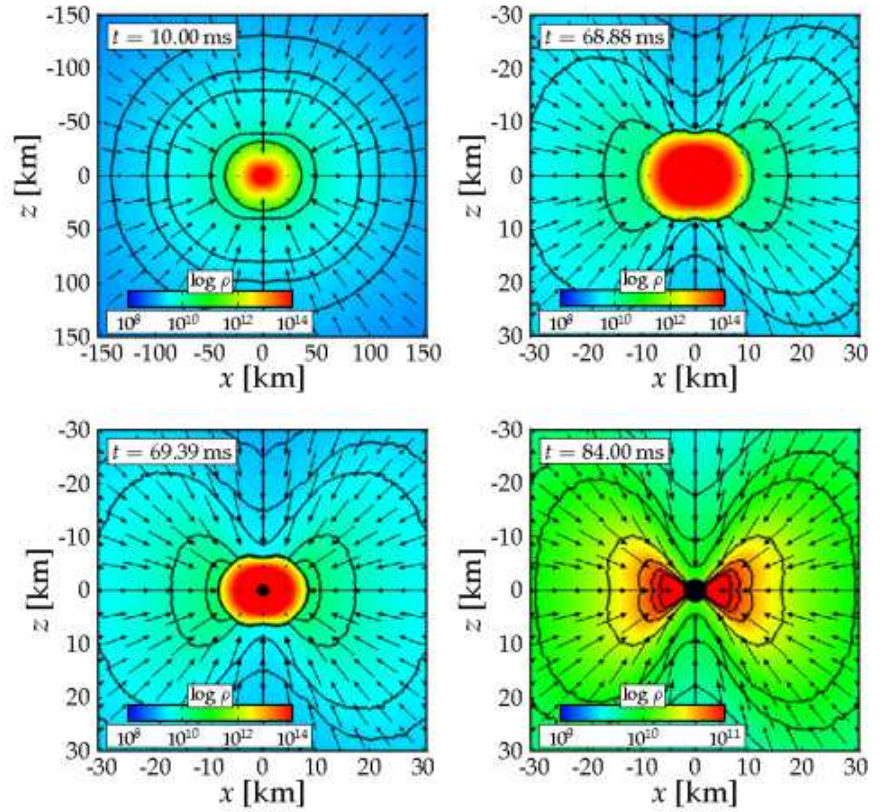


Figure 8: Density colormaps of the meridional plane of a collapsing $75M_{\odot}$ star, superposed with velocity vectors at various times after bounce (and note the different scale of the top left panel from the rest). The collapse first forms a proto-neutron star (top panels) which later collapses to a BH (bottom panels). (From (172)).